

Scaling and Load-Balancing Equi-Joins

Ahmed Metwally
Uber, Inc.
Sunnyvale, CA, USA
ametwally@uber.com

ABSTRACT

The task of joining two tables is fundamental for querying databases. In this paper, we focus on the equi-join problem, where a pair of records from the two joined tables are part of the join results if equality holds between their values in the join column(s). While this is a tractable problem when the number of records in the joined tables is relatively small, it becomes very challenging as the table sizes increase, especially if hot keys (join column values with a large number of records) exist in both joined tables.

This paper, an extended version of [53], proposes Adaptive-Multistage-Join (AM-Join) for scalable and fast equi-joins in distributed shared-nothing architectures. AM-Join utilizes (a) Tree-Join, a proposed novel algorithm that scales well when the joined tables share hot keys, and (b) Broadcast-Join, the known fastest when joining keys that are hot in only one table.

Unlike the state-of-the-art algorithms, AM-Join (a) holistically solves the join-skew problem by achieving load balancing throughout the join execution, and (b) supports all outer-join variants without record deduplication or custom table partitioning. For the fastest AM-Join outer-join performance, we propose the Index-Broadcast-Join (IB-Join) family of algorithms for Small-Large joins, where one table fits in memory and the other can be up to orders of magnitude larger. The outer-join variants of IB-Join improves on the state-of-the-art Small-Large outer-join algorithms.

The proposed algorithms can be adopted in any shared-nothing architecture. We implemented a MapReduce version using Spark. Our evaluation shows the proposed algorithms execute significantly faster and scale to more skewed and orders-of-magnitude bigger tables when compared to the state-of-the-art algorithms.

1. INTRODUCTION

Retrieval of information from two database tables is critical for data processing, and impacts the computational cost and the response time of queries. In the most general case, this operation entails carrying out a cross join of the two tables. The more common case is computing an equi-join, where two records in the two tables are joined if and only if equality holds between their *keys* (values in the join column(s)). The algorithms for equi-joins have been optimized regularly since the inception of the database community [27, 70, 14, 25, 31, 35, 68, 47, 71, 34].

Significant research has been done to enhance the sequential equi-join algorithms on multi-core processors [45, 16, 4, 9, 8, 69, 12, 10] and on GPUs [41, 44, 20, 39, 72, 58, 65, 59]. However, the proliferation of data collection and analysis poses a challenge to sequential join algorithms that are limited by the number of threads supported by the processing units. Scaling equi-joins had to progress through distributed architectures, which is the direction adopted in this work.

This work is motivated by equi-joining industry-scale skewed datasets in a novel way. We introduce *same-attribute self-joins* at the intersection of equi-joins [28], inner-joins, and self-joins [42]. This novel join semantic is an integral operation in the similarity-based join algorithms (e.g., [55]) used for fraud detection. While same-attribute self-joins can be more efficient to perform than the general equi-joins, the state-of-the-art equi-join algorithms failed to scale to our large and skewed datasets. This motivated us to develop the fast, efficient, and scalable Adaptive-Multistage-Join (AM-Join) that scales, not only to our specialized use case, but also to the most challenging equi-joins.

We first propose Tree-Join, a novel algorithm that scales well by distributing the load of joining a key that is *hot* (i.e., high-frequency or shared by a large number of records) in both tables to multiple executors. Such keys are the scalability bottleneck of most of the state-of-the-art distributed algorithms. We give special attention to balancing the load among the executors throughout the Tree-Join execution.

We then tackle Small-Large joins, where one table fits in memory and the other can be up to orders of magnitude larger. We devise the Index-Broadcast-Join (IB-Join) family for Small-Large joins, and show analytically their outer-join variants improve on the state-of-the-art Small-Large outer-join algorithms [78, 24].

The Tree-Join, and the Broadcast-Join algorithms are the building blocks of AM-Join. AM-Join achieves (a) high scalability by utilizing Tree-Join that distributes the load of joining a key that is hot in both relations to multiple executors, and (b) fast execution by utilizing the Broadcast-Join algorithms that reduce the network load when joining keys that are hot in only one relation. AM-Join extends to all outer-joins elegantly without record deduplication or custom table partitioning, unlike the state-of-the-art industry-scale algorithms [19]. The outer-join variants of AM-Join achieves fast execution by utilizing the IB-Join family of algorithms.

All the proposed algorithms use the basic MapReduce primitives only, and hence can be adopted on any shared-nothing architecture. We implemented a MapReduce version using Spark [82]. Our evaluation highlights the im-

Symbol	Meaning
\mathcal{R}, \mathcal{S}	The joined relations/tables.
Q	The relation/table storing the join results.
b	The join attribute(s)/column(s).
ℓ	The number of records, a.k.a., frequency, with a specific key in either \mathcal{R} or \mathcal{S} .
ℓ_{max}	The maximum value of ℓ .
λ	The relative cost/runtime of sending data over the network vs. its IO from/to a local disk. $\lambda \geq 0$.
ℓ'	For a given key, the number of records a subsequent Tree-Join executor receives, where $\ell' = \ell^p$, for some p , s.t. $0 \leq p \leq 1$.
$\delta(\ell)$	The number of sub-lists produced by the splitter in Tree-Join for a list of length ℓ .
t	The number of iterations of Tree-Join.
$\kappa_{\mathcal{R}}, \kappa_{\mathcal{S}}$	The hot keys in \mathcal{R} and \mathcal{S} .
$ \kappa_{\mathcal{R}} _{max}, \kappa_{\mathcal{S}} _{max}$	The maximum numbers of hot keys collected for \mathcal{R} and \mathcal{S} .
M	The available memory per executor.
m_{id}	The size of a record identifier.
m_b	The average size of a b key.
$m_{\mathcal{R}}, m_{\mathcal{S}}$	The average size of records in \mathcal{R} and \mathcal{S} .
$\Delta_{operation}$	The expected runtime of <i>operation</i> .
n	The number of executors.
e_i	A specific executor.
$\mathcal{R}_i, \mathcal{S}_i$	The partitions of \mathcal{R} and \mathcal{S} on e_i .

Table 1: The symbols used in the paper.

proved performance and scalability of AM-Join when applied to the general equi-joins. When compared to the state-of-the-art algorithms [19, 36], AM-Join executed comparably fast on weakly-skewed synthetic tables and can join more-skewed or orders-of-magnitude bigger tables, including our real-data tables. These advantages are even more pronounced when applying the join algorithms to same-attribute self-joins. The proposed IB-Join outer-join algorithm executed much faster than the algorithms in [78, 24].

The rest of the paper is organized as follows. We formalize the problem, propose same-attribute self-joins and lay out the necessary background in § 2. We review the related work in § 3. We propose Tree-Join in § 4. We then discuss Small-Large joins and propose Index-Broadcast-Join in § 5. The Adaptive-Multistage-Join is described in § 6. In § 7, we discuss identifying hot keys, which is an integral part of Adaptive-Multistage-Join. We report our evaluation results in § 8, and summarize our contributions in § 9.

2. FORMALIZATION

We now introduce the concepts used. As the readers progress through the paper, they are referred to Table. 1 for the symbols used.

2.1 Equi-Joins, Inner-Joins and Self-Joins

The equi-join operation combines columns from two tables, a.k.a. relations in the relational database community, based on the equality of the column(s), a.k.a., join attribute(s). We focus on the case where two relations are joined. Other work, e.g., [2, 56, 26, 1], focused on extending equi-joins to multiple relations.

Given two relations \mathcal{R} and \mathcal{S} , where $\mathcal{R} = (a, b)$ and $\mathcal{S} = (b, c)$, the equi-join results in a new relation $Q = (a, b, c)$, where b is the join attribute(s), and a and c are the remaining attribute(s) from \mathcal{R} and \mathcal{S} , respectively. Any pair of records, r from \mathcal{R} and s from \mathcal{S} whose b attribute(s) have equal values, i.e., $r(b) = s(b)$, is output to Q . This is captured by the notation $Q = \mathcal{R} \bowtie_{r(b)=s(b)} \mathcal{S}$ or by the shorter notation $Q = \mathcal{R} \bowtie_b \mathcal{S}$.

In case a record in \mathcal{R} or \mathcal{S} is output to Q if and only if its b attribute(s) do have a match on the other side of the join, this is called an *inner-join*. If a record in \mathcal{R} (\mathcal{S}) is output to Q whether or not it has a match on its b attribute(s) in \mathcal{S} (\mathcal{R}), this is called a *left-outer-join* (*right-outer-join*). If any record in \mathcal{R} or \mathcal{S} is output to Q even if its b attribute(s) do not have a match on the other side of the join, this is called a *full-outer-join*. Fig. 1 shows an example of joining the two relations, \mathcal{R} and \mathcal{S} , shown in Fig. 1(a). The results of the inner, left-outer, right-outer, and full-outer-joins are shown in Fig. 1(b) through Fig. 1(e), respectively.

In case \mathcal{R} and \mathcal{S} are the same table, this is called *self-join* [42]. A table can be self-joined using different join attributes, b_1 and b_2 on the two sides of the join, captured by the notation $\mathcal{R} \bowtie_{r_1(b_1)\theta r_2(b_2)} \mathcal{R}$, where θ is the function that has to hold between the b_1 and b_2 attribute(s) of records r_1 and r_2 respectively for the pair r_1 - r_2 to belong to Q . If the same join attributes are used on both sides of the self-join, i.e., $b_1 = b_2 = b$, and θ is the equality function, i.e., the join condition is $r_1(b) = r_2(b)$, then this is an inner-join by definition, and is captured by the notation $\mathcal{R} \bowtie_{r_1(b)=r_2(b)} \mathcal{R}$, or $\mathcal{R} \bowtie_b \mathcal{R}$ for short. We call this special case *same-attribute self-join*. The Q produced by a same-attribute self-join contains duplicate pairs of records, but in reverse order. To eliminate the redundancy in Q , we drop the join completeness: (a) a pair $r - r$ should be in Q exactly once, and (b) a pair r_2 - r_1 should not be in Q , if $r_1 \neq r_2$ and r_1 - r_2 is in Q .

2.2 Popular Distributed-Processing Frameworks

MapReduce [32] is a popular framework with built-in fault tolerance. It allows developers, with minimal effort, to scale data-processing algorithms to shared-nothing clusters, as long as the algorithms can be expressed in terms of the functional programming primitives *mapRec* and *reduceRecs*.

$$mapRec : \langle key_1, value_1 \rangle \rightarrow \langle key_2, value_2 \rangle^*$$

$$reduceRecs : \langle key_2, value_2^* \rangle \rightarrow value_3^*$$

The input dataset is processed using *executors* that are orchestrated by the *driver* machine. Each record in the dataset is represented as a tuple, $\langle key_1, value_1 \rangle$. Initially, the dataset is partitioned among the *mappers* that execute the map operation. Each mapper applies *mapRec* to each input record to produce a potentially-empty list of the form $\langle key_2, value_2^* \rangle^*$. Then, the *shufflers* group the output of the mappers by the key. Next, each *reducer* is fed a tuple of the form $\langle key_2, value_2^* \rangle$, where $value_2^*$, the *reduce_value_list*, contains all the $value_2$'s that were output by any mapper with the key_2 . Each reducer applies *reduceRecs* on the $\langle key_2, value_2^* \rangle$ tuple to produce a potentially-empty list of the form $value_3^*$. Any MapReduce job can be expressed as the lambda expression below.

MapReduce(dataset) :

$$dataset.map(mapRec).groupByKey.reduce(reduceRecs)$$

In addition to key_2 , the mapper can optionally output tuples by a secondary key. The *reduce_value_list* would also be sorted by the secondary key in that case¹. Partial reducing

¹Secondary keys are not supported by the public version of MapReduce, Hadoop [6]. Two ways to support secondary

\mathcal{R}		\mathcal{S}		\mathcal{Q}_{Inner}			$\mathcal{Q}_{Left-Outer}$			$\mathcal{Q}_{Right-Outer}$			$\mathcal{Q}_{Full-Outer}$		
key	rec _R	key	rec _S	key	rec _R	rec _S	key	rec _R	rec _S	key	rec _R	rec _S	key	rec _R	rec _S
1	"a"	1	"q"	1	"a"	"q"	1	"a"	"q"	1	"a"	"q"	1	"a"	"q"
1	"w"	1	"z"	1	"w"	"q"	1	"w"	"q"	1	"w"	"q"	1	"w"	"q"
2	"d"	4	"h"	1	"a"	"z"	1	"a"	"z"	1	"a"	"z"	1	"a"	"z"
2	"h"	5	"f"	1	"w"	"z"	1	"w"	"z"	1	"w"	"z"	1	"w"	"z"
3	"f"	6	"f"	4	"a"	"h"	2	"d"	null	4	"a"	"h"	2	"d"	null
3	"g"	6	"y"	4	"c"	"h"	2	"h"	null	4	"c"	"h"	2	"h"	null
4	"a"	7	"k"	5	"a"	"f"	3	"f"	null	5	"a"	"f"	3	"f"	null
4	"c"	8	"c"	6	"a"	"f"	3	"g"	null	6	"a"	"f"	3	"g"	null
5	"a"	9	"e"	6	"a"	"y"	4	"a"	"h"	6	"a"	"y"	4	"a"	"h"
6	"a"	11	"a"	7	"e"	"k"	4	"c"	"h"	7	"e"	"k"	4	"c"	"h"
7	"e"	11	"p"	8	"b"	"c"	5	"a"	"f"	8	"b"	"c"	5	"a"	"f"
8	"b"	12	"c"	9	"a"	"e"	6	"a"	"f"	9	"a"	"e"	6	"a"	"f"
9	"a"	12	"h"	9	"a"	"e"	6	"a"	"y"	11	null	"a"	6	"a"	"y"
10	"d"	13	"v"				7	"e"	"k"	11	null	"p"	7	"e"	"k"
							8	"b"	"c"	12	null	"c"	8	"b"	"c"
							9	"a"	"e"	12	null	"h"	9	"a"	"e"
							10	"d"	null	13	null	"v"	10	"d"	null
													11	null	"a"
													11	null	"p"
													12	null	"c"
													12	null	"h"
													13	null	"v"

Figure 1: An example for joining two relations. (a) shows the input relations. (b) through (e) show the results of the inner, left-outer, right-outer, and full-outer-joins, respectively. The tables are sorted for readability, but sorting is not guaranteed in practice.

can happen at the mappers, which is known as *combining* to reduce the network load. For more flexibility, the MapReduce framework allows for loading external data when mapping or reducing. However, to preserve the determinism and the purity of the *mapRec* and *reduceRecs* functions, loading is restricted to the beginning of each operation.

The Spark framework [82] is currently the *de facto* industry standard for distributing data processing on shared-nothing clusters. Spark offers the functionality of MapReduce², as well as convenience utilities that are not part of MapReduce, but can be built using MapReduce. One example is performing tree-like aggregation of all the records in a dataset [48]. The *treeAggregate* operation can be implemented using a series of MapReduce stages, where each stage aggregates the records in a set of data partitions, and the aggregates are then aggregated further in the next stage, and so on, until the final aggregate is collected at the driver.

Spark supports other functionalities that cannot be implemented using the map and reduce operations. One example is performing hash-like lookups on record keys over the network. These Spark-specific functionalities perform well under the assumption the dataset partitions fit in the memory of the executors.

3. RELATED WORK

We review the distributed algorithms that are generally applicable to equi-joins, and those targeting Broadcast outer-joins. We only review equi-joins in homogenous shared-nothing systems, where the processing powers of the execu-

keys were proposed in [51]. The first entails loading the entire *reduce_value_list* in the reducer memory, and the second entails rewriting the shuffler. The second solution is more scalable but incurs higher engineering cost.

²While Spark uses the same nomenclature of MapReduce, the MapReduce map function is called *flatMap* in Spark. We use the MapReduce notation, introduced in [32].

tors are comparable. We neither review the algorithms devised for heterogenous architectures (e.g., [75]) nor in streaming systems (e.g., [30, 38, 50]), nor the approximate equi-join algorithms (e.g., [62]).

3.1 General Distributed Equi-Joins

The work most relevant to ours is that of distributing equi-joins on MapReduce [32] and on general shared-nothing [73] architectures.

3.1.1 MapReduce Equi-Joins

The seminal work in [17] explained *Map-Side* join (a.k.a., *Broadcast* or *Duplication* join in the distributed-architecture community), which is discussed in more details in § 5. This work also extended the Sort-Merge join [18] to the MapReduce framework. It also proposed using secondary keys to alleviate the bottleneck of loading the records from both joined relations in memory. This Sort-Merge join is considered a *Reduce-Side* join (a.k.a., *Shuffle* join in the distributed-architecture community). However, the work in [17] overlooks the skew in key popularity.

The SAND Join [7] extends the Reduce-Side joins by partitioning data across reducers based on a sample. The work in [57] improves this key-range partitioning using quantile computation. It extends key-range partitioning to combinations of keys in the join results, and maps combinations of keys to specific reducers to achieve load-balancing. The algorithms in [76, 36] use sampling to build the cross-relation histogram, and balance the load between the executors based on the sizes of the relations and the estimated size of the join results.

There are major drawbacks with these key-range-division approaches [7, 57, 76, 36]. In the pre-join step, the key-range computation and communication over the network to the mappers incurs significant computational [21] and communication cost [81]. The computational and network bottlenecks are more pronounced when computing key-ranges

for combinations of attributes [57]³. These approaches implicitly assume that the keys are distributed evenly within each key range, which is rarely true for highly-diverse key spaces, highly-skewed data, or practical bucket sizes.

3.1.2 Shared-Nothing Equi-Joins

The algorithm in [40] is similar to that in [57] discussed above. It allows for grouping the records into evenly distributed groups that are executed on individual executors. However, it suffers from the same hefty overhead.

Map-Reduce-Merge [80] extends MapReduce with a *merge* function to facilitate expressing the join operation. Map-Join-Reduce [43] adds a join phase between the map and the reduce phases. These extensions cannot leverage the MapReduce built-in fault tolerance, and are implemented using complicated custom logic.

The Partial Redistribution & Partial Duplication (PRPD) algorithm in [79] is a hybrid between hash-based [46, 33] (as opposed to Sort-Merge [37, 9, 13]) and duplication-based join algorithms [34]. The PRPD algorithm collects $\kappa_{\mathcal{R}}$, and $\kappa_{\mathcal{S}}$, the hot (a.k.a. high-frequency) keys in \mathcal{R} and \mathcal{S} , respectively. For the correctness of the algorithm, a key that is hot in both \mathcal{R} and \mathcal{S} is only assigned to either $\kappa_{\mathcal{R}}$ or to $\kappa_{\mathcal{S}}$. PRPD splits \mathcal{S} into (a) \mathcal{S}_{high} with keys in $\kappa_{\mathcal{S}}$, whose records are not distributed to the executors, (b) \mathcal{S}_{dup} with keys in $\kappa_{\mathcal{R}}$, whose records are broadcasted to all the executors containing \mathcal{R}_{high} records, and (c) \mathcal{S}_{hash} the remaining records that are distributed among executors using hashing. \mathcal{R} is split similarly into \mathcal{R}_{high} , \mathcal{R}_{dup} , and \mathcal{R}_{hash} . \mathcal{S}_{hash} is joined with \mathcal{R}_{hash} on the executors they were hashed into, and \mathcal{S}_{high} (\mathcal{R}_{high}) is joined with \mathcal{R}_{dup} (\mathcal{S}_{dup}) on the executors containing \mathcal{S}_{high} (\mathcal{R}_{high}). The union of the three joins comprise the final join results.

Track-Join [60] aims at minimizing the network load using a framework similar to PRPD. For any given key, Track-Join migrates its records from one relation to a few executors [61], and *selectively broadcasts*, i.e., multicasts, the records from the other relation to these executors. This record migration process is expensive. Moreover, identifying the executors on which the join takes place is done in a preprocessing *track* phase, which is a separate distributed join that is sensitive to skew in key popularity.

The PRPD algorithm is developed further into the SkewJoin algorithm in [19]. Three flavors of SkewJoin are proposed. The Broadcast-SkewJoin (BSJ) is the same as PRPD. On the other end of the spectrum, Full-SkewJoin (FSJ) distributes \mathcal{S}_{high} and \mathcal{R}_{high} in a round-robin fashion on the executors using a specialized partitioner. This offers better load balancing at the cost of higher distribution overhead. The Hybrid-SkewJoin (HSJ) is a middle ground that retains the original data partitioning on the non-skewed side.

The PRPD algorithm is extended by [23] to use distributed lookup servers⁴. However, the algorithm in [23] splits \mathcal{S} into \mathcal{S}_{hash} and \mathcal{S}_{high} . \mathcal{S}_{hash} , along with the distinct keys of \mathcal{S}_{high} , are hashed into the executors. All \mathcal{R} is hashed into the executors. On each executor, e_i , \mathcal{R}_i is joined with \mathcal{S}_{hash_i} , and with \mathcal{S}_{high_i} . The results of joining \mathcal{R}_i with \mathcal{S}_{hash_i} are reported as part of the final results. The results

of joining \mathcal{R}_i with \mathcal{S}_{high_i} are augmented with the right \mathcal{S} records using the distributed lookup servers.

Flow-Join [63] is similar to PRPD, but it detects the hot keys while performing the cross-network join. Flow-Join utilizes (a) *Remote Direct Memory Access* (RDMA) [49] over high-speed network [64, 15, 66] and (b) work-stealing across cores and Non-Uniform Memory Access (NUMA) [64] regions for local processing on rack-scale systems.

3.1.3 Comments on the General Distributed Equi-Joins

MapReduce is more restrictive than Spark that supports distributed lookups, for example. Spark is more restrictive than the general shared-nothing architecture that supports multicasting data, for example. An algorithm proposed for a more restrictive environment can be adopted for a less restrictive one, but the opposite is not true.

All the above algorithms that mix Broadcast-Joins and Shuffle-Joins [79, 60, 61, 19, 23, 63] do not extend smoothly to the outer-join variants. Mixing these two join techniques in the PRPD fashion results in having *dangling tuples* (tuples that do not join on the other side) of the same key distributed across the network. Deduplicating and counting dangling tuples across the network is a non-trivial operation, and was only discussed in [19, 63].

The strongest bottleneck in the Shuffle-Join (Hash or Sort-Merge) algorithms is they assume the Cartesian product of the records of any given key is computed using one executor. Hence, they fail to handle highly skewed data, where one key can bottleneck an entire executor. Consequently, all the other executors remain under-utilized while waiting for the bottleneck executor to finish [74].

On the other hand, the strongest drawback of all the algorithms that use Broadcast-Join is low scalability when there exist keys that are hot in both of the joined relations. In such cases, the broadcasted keys are hot, and their records may not fit in memory. Even if the records of the hot keys may fit in memory, the entire broadcasted relation may not fit in memory. Moreover, the computational load of joining hot keys is only balanced if the non-duplicated hot keys are evenly distributed among the executors.

3.2 Small-Large Outer-Joins

We now discuss the outer-joins when one relation can fit in memory and the other is orders of magnitude larger. Broadcast-Joins are the fastest-known for these *Small-Large join cases*. A solution to this problem is essential for extending AM-Join to outer-joins.

For a left-outer-join, the Duplication and Efficient Redistribution (DER) algorithm [78] broadcasts the small relation, \mathcal{S} , to all n executors. On each executor, e_i , \mathcal{S} is inner joined with \mathcal{R}_i . The joined records are output, and the ids of the *unjoined* records of \mathcal{S} are distributed to the n executors based on their hash. If an executor receives n copies of a record id, then this \mathcal{S} id is *unjoinable* with \mathcal{R} (since it was unjoined on the n executors). The unjoinable ids are inner Hash-Joined with \mathcal{S} and *null*-padded. The left-outer-join result is the union of the two inner join results.

The Duplication and Direct Redistribution (DDR) algorithm [24] is similar to DER, but for the records failing the first inner join, each executor hashes the entire unjoined record, instead of only its id, over the network. Because entire records, instead of their ids, are hash-distributed, (a)

³This problem was the focus of [5] in the context of estimating join results size.

⁴Utilization lookup servers has been proposed before by the same research group [22].

the first join can be executed as an out-of-the-box left-outer-join, and (b) the second inner join is not needed. Extending DER and DDR to full-outer-joins is achieved by changing the first join to output the unjoined records on \mathcal{R}_i .

4. THE TREE-JOIN ALGORITHM

As a first step towards AM-Join, we first propose Tree-Join, a novel algorithm that can execute over multiple stages, each corresponding to a MapReduce Job. Tree-Join scales well even in the existence of keys that are hot in both of the joined relations. If a Shuffle-Join (Hash or Sort-Merge) is executed, a bottleneck happens because a single executor has to process and output a disproportionately large number of pairs of records that have the same hot key. Tree-Join, on the other hand, alleviates this bottleneck by utilizing the idle executors without doing any duplicate work, while adding minimal overhead.

We start by describing the basic algorithm in § 4.1, we then take the first step towards load-balancing in § 4.2, and describe the final load-balanced algorithm in § 4.3. We discuss handling same-attribute self-joins in § 4.4. We analyze some of the algorithm parameters in § 4.5, and establish the execution stages are very limited in number in § 4.6.

Algorithm 1 *treeJoinBasic*(\mathcal{R}, \mathcal{S})

Input: Two relations to be joined.
Output: The join results.
1: $joined_index = buildJoinedIndex(\mathcal{R}, \mathcal{S})$
2: $\mathcal{Q} = \text{empty Dataset}$
3: **while** $joined_index.nonEmpty$ **do**
4: $\langle partial_results, new_index \rangle =$
 $treeJoinIteration(joined_index)$
5: $\mathcal{Q} = \mathcal{Q} \cup partial_results$
6: $joined_index = new_index.randomShuffle$
7: **end while**
Return \mathcal{Q}

4.1 The Basic Tree-Join Algorithm

We start by describing a basic version of the inner variant of Tree-Join (Alg. 1). The outer-join variants are straightforward extensions. The algorithm starts by building a distributed *joined index* (Alg. 2). This is done by hashing the records of the two relations based on their keys using the same hash function into the different partitions of the joined index. Hence, the records of each key from both relations end up in the same partition.

Each key in the joined index has two *joined lists* of records, one list coming from each relation. The keys are joined independently, and the union of their join results constitutes the join results of \mathcal{R} and \mathcal{S} . This *key-independence* observation simplifies the analysis in § 4.2 and onwards.

The keys are joined in stages, i.e., iteratively. In each iteration (Alg. 3), each partition of the joined index is split locally by the executor into two partitions, the cold partition and the hot partition (Line 1 in Alg. 3). If the joined lists of a key are short enough (based on the analysis in § 4.5), the key is cold and it belongs to the cold partition. The join results of this key are obtained by outputting the key with all pairs of records from both relations (Line 2 in Alg. 3). However, if the record lists are long, the key is hot, and it belongs to the hot partition. The executor processing this partition acts as a *splitter* for the key. The executor chunks each of the two joined lists into sub-lists (Line 4 in Alg. 3), and outputs all pairs of sub-lists (Line 5 in Alg. 3). This dataset of pairs

of sub-lists produced from the hot partitions constitutes the joined index to be processed in the next iteration. In the next iteration, the keys and their pairs of joined lists are assigned to random partitions to distribute the load among the executors (Line 6 in Alg. 1).

Fig. 2 shows an example of *treeJoinBasic* (Alg. 1). The *buildJoinedIndex* algorithm (Alg. 2) is invoked to build the initial joined index, $joined_index_0$ (Fig. 2(b)), on the input relations in Fig. 2(a). Notice that all the keys in this initial index are distinct. Assuming that any key whose joined lists has 2 or fewer records in both joined relations is considered cold, the joined lists of keys 3 and 4 are used to produce the first partial results, $partial_results_1$ (Fig. 2(c)) and the joined lists of keys 1 and 2 are chunked into the first joined index, $joined_index_1$ (Fig. 2(d)), and the joined lists of keys 5 and 6 are discarded, since they have records in only one relation.

$map_{buildJoinedIndex}$:

$$r_i \rightarrow \langle key_{r_i}, \langle 0, r_i \rangle \rangle$$

$$s_j \rightarrow \langle key_{s_j}, \langle 1, s_j \rangle \rangle$$

$reduce_{buildJoinedIndex}$:

$$\langle key, (\langle 0, r_i \rangle \text{ OR } \langle 1, s_j \rangle)^* \rangle \rightarrow \langle key, r_i^*, s_j^* \rangle$$

Algorithm 2 *buildJoinedIndex*(\mathcal{R}, \mathcal{S})

Input: Two relations to be joined.
Output: A joined index mapping each key to the pair of lists of records.
1: $keyed_r = \mathcal{R}.map(map_{buildJoinedIndex})$
2: $keyed_s = \mathcal{S}.map(map_{buildJoinedIndex})$
3: $joined_index = keyed_r$
4: $.union(keyed_s)$
5: $.groupByKey$
6: $.reduce(reduce_{buildJoinedIndex})$
Return $joined_index$

Notice that the keys in $joined_index_1$ are repeated. Line 6 in Alg. 1 distributes these keys randomly among the executors for load balancing. *treeJoinIteration* (Alg. 3) uses the keys that have 2 or fewer records in both joined relations in $joined_index_1$ to produce the second partial results, $partial_results_2$ (Fig. 2(e)), and uses the remaining keys to produce the second joined index, $joined_index_2$ (Fig. 2(f)). While all the keys in $joined_index_2$ have the same value, they are distributed among the executors for load balancing. All the keys in $joined_index_2$ have 2 or fewer records in both joined relations. Hence, no more iterations are executed, and $joined_index_2$ is used to produce the third and final partial result, $partial_results_3$ (Fig. 2(g)). The union of the three partial results constitutes the inner-join results of the input relations in Fig. 2(a).

$map_{chunkPairOfLists}$:

$$\langle key, \mathcal{L}_1, \mathcal{L}_2 \rangle \rightarrow \langle key, chunkList(\mathcal{L}_1), chunkList(\mathcal{L}_2) \rangle$$

We next analyze *treeJoinBasic*. For simplicity, we assume both lists of a joined key have the same length, ℓ , and λ is the relative cost of sending data over the network vs. its IO from/to a local disk, and $\lambda > 0$.

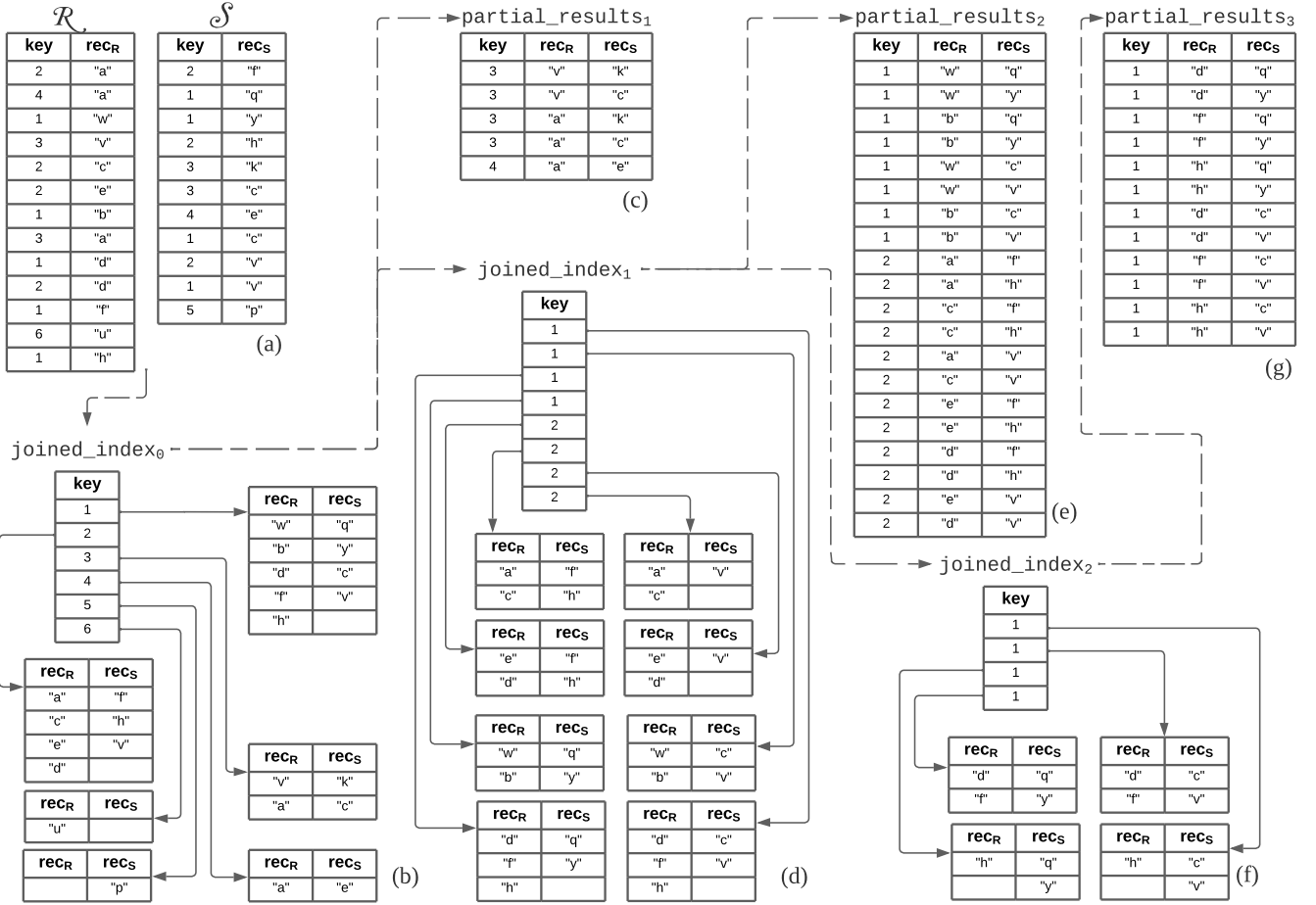


Figure 2: An example of inner-joining two relations using *treeJoinBasic*. (a) The input relations. (b) The initial index built from the input relations in (a). The initial index is used to produce (c) the first partial results, and (d) the first joined index. The first joined index is used to produce (e) the second partial results, and (f) the second joined index. The second joined index is used to produce (g) the third partial results. The union of the partial results in (c), (e), and (g) constitutes the inner-join results.

Algorithm 3 *treeJoinIteration*(*joined_index*)

Input: A joined index of two relations to be joined.

Output: Join results of some keys, and the joined index (of the remaining keys) for next iteration.

```

1:  $\langle \text{cold\_index}, \text{hot\_index} \rangle = \text{splitPartitionsLocally}(\text{joined\_index}, \text{isHotKey})$ 
2:  $\text{partial\_results} = \text{cold\_index.map}(\text{map\_getAllValuePairs})$ 
3:  $\text{new\_index} = \text{hot\_index}$ 
4:    $\text{.map}(\text{map\_chunkPairOfLists})$ 
5:    $\text{.map}(\text{map\_getAllValuePairs})$ 
   Return  $\langle \text{partial\_results}, \text{new\_index} \rangle$ 

```

Algorithm 4 *map_getAllValuePairs*($\langle \text{key}, \mathcal{L}_1, \mathcal{L}_2 \rangle$)

Input: A tuple of the key, and two lists.

Output: A list of triplets, each triplet has *key* and a pair from \mathcal{L}_1 and \mathcal{L}_2 . All pairs from \mathcal{L}_1 and \mathcal{L}_2 are output.

```

1:  $u = \text{empty Buffer}$ 
2: for all  $v_i \in \mathcal{L}_1, v_j \in \mathcal{L}_2$  do
3:    $u.\text{append}(\langle \text{key}, v_i, v_j \rangle)$ 
4: end for
   Return  $u$ 

```

4.2 Chunking Lists of Hot Keys

Computing the optimal number of sub-lists for a list of records is crucial for load balancing between the executors and across iterations. Chunking a pair of joined lists into numerous pairs of sub-lists adds overhead to the splitter, the executor assigned the original pair of lists. Conversely, chunking the pair of joined lists into few pairs of sub-lists adds overhead to the executors that handle these pairs in the subsequent iteration.

We choose to balance the load between any splitter at any iteration and the subsequent executors that process its key. Ignoring the key size, for each of the joined lists, the splitter produces $\delta(\ell) = \ell/\ell^p = \ell^{1-p}$ sub-lists, each is of size $\ell' = \ell^p$, for some p , where $0 \leq p \leq 1$. The splitter outputs $\Theta((\ell^{1-p})^2)$ pairs of sub-lists. Hence, the output of this executor is $\Theta(\ell^{2-2p})$ pairs of sub-lists, each containing ℓ' records. Therefore, the splitter work is $\Theta(\ell^{2-p})$ records. Each subsequent executor receiving a pair of sub-lists outputs $\Theta((\ell')^2)$ pairs of records. Hence, the output of each subsequent executor is $\Theta(\ell^{2p})$ records. To achieve decent load balancing between the splitter and each subsequent executor, the loads should be comparable, yielding $2 - p = 2p$.

$$p = \frac{2}{3} \quad (1)$$

From Eqn. 1, to achieve the load-balancing goal, $\delta(\ell)$, the number of sub-lists is $\lceil \sqrt[3]{\ell} \rceil$, and each has $\lceil \ell^{\frac{2}{3}} \rceil$ records, as shown in Alg. 5.

To illustrate using an example, assuming two joined lists each has 10^5 records. A naïve Shuffle-Join would output 10^{52} pairs of records, i.e., 2×10^{10} IO, using one executor. Meanwhile, the *treeJoinBasic* splitter would chunk each list into 47 sub-lists, and would output $47 \times 47 \times (2128 + 2128)$ records, which is $\approx 9.4 \times 10^6$ IO. Each one among the 2209 subsequent executors would output $2128 \times 2128 \times 2 \approx 9.1 \times 10^6$ IO. Notice the only overhead for utilizing 2209 executors to process the join of this key is producing $\approx 9.4 \times 10^6$ IO by the splitter, and sending this data over the network. Since $\frac{9.4 \times 10^6}{2 \times 10^{10}} < 0.05\%$, this overhead is $\approx (1 + \lambda) \times 0.05\%$. If the lists instead had 10^4 (10^3) records, the load can be distributed on 484 (100) executors, and the overhead would only increase to $(1 + \lambda) \times 0.2\%$ ($(1 + \lambda) \times 1\%$).

Algorithm 5 *chunkList*(\mathcal{L})

Input: A list of records.

Output: A list of sub-lists of records.

```

1:  $\ell = |\mathcal{L}|$  // The length of  $\mathcal{L}$ .
2:  $\delta(\ell) = \lceil \sqrt[3]{\ell} \rceil$  // The number of sub-lists.
3:  $\ell' = \lceil \ell^{\frac{2}{3}} \rceil$  // The length of a sub-list.
Return  $[\mathcal{L}_0 \dots \mathcal{L}_{\ell'-1}], [\mathcal{L}_{\ell'} \dots \mathcal{L}_{2 \times \ell'-1}], \dots, [\mathcal{L}_{(\delta(\ell)-1) \times \ell'} \dots \mathcal{L}_C]$ 

```

4.3 The Fully-Balanced Tree-Join Algorithm

The *treeJoinBasic* algorithm (§ 4.1) and optimal list-chunking (§ 4.2) achieve load balancing and good resource utilization. However, this is only true once the initial joined index has been built, and the first-iteration splitters are done splitting the joined lists of the hot keys (Lines 1 and 4 of Alg. 1). However, these early operations suffer from load imbalance, since early executors handle complete lists of hot keys. A first-iteration executor that is assigned a hot key may (a) have higher splitting load than other splitters in the first-iteration, and (b) not be able to fit all the records of that hot key in its memory to perform the splitting, resulting in thrashing and hence throttling the join [74]. To achieve maximal load balancing among the executors building the initial joined index, and performing the first-iteration splitting, we identify hot keys, and give their records some special treatment before adding them to the initial joined index.

As a preprocessing step, hot keys are identified using the approximate distributed heavy-hitters algorithm in [3]. We only discuss \mathcal{R} , but the logic applies to \mathcal{S} . The algorithm runs the local Space-Saving algorithms [54] on individual \mathcal{R} partitions, and then merges the local results. We can do the merging over the network in a tree-like manner using a priority queue of bounded size, $|\kappa_{\mathcal{R}}|_{max}$, where $|\kappa_{\mathcal{R}}|_{max}$ is the number of hot keys to be collected from \mathcal{R} ⁵. If \mathcal{R} is already partitioned by the key, all records of any key reside on one partition, and its local frequency is equal to its global

frequency. In that case, this technique would find the hot keys exactly.

The load-balanced version of Tree-Join is formalized in Alg. 6. The hot keys in both \mathcal{R} and \mathcal{S} and their corresponding frequencies are identified in Lines 1 and 2, respectively. Their frequency maps, $\kappa_{\mathcal{R}}$ and $\kappa_{\mathcal{S}}$, are joined in Line 3 yielding $\kappa_{\mathcal{RS}}$, a map from each shared hot key to a tuple of two numbers: the key frequencies in \mathcal{R} and \mathcal{S} , respectively. $\kappa_{\mathcal{RS}}$ is then broadcasted to all executors to be cached and used later for local processing.

\mathcal{R} is split into \mathcal{R}_H , a sub-relation that contains only the \mathcal{R} records with keys in $\kappa_{\mathcal{RS}}$, and \mathcal{R}_C , a sub-relation that contains the records whose keys are not in $\kappa_{\mathcal{RS}}$ (Line 5). \mathcal{S} is split similarly into \mathcal{S}_H and \mathcal{S}_C (Line 6). The cold sub-relations are used to build a cold joined index (Line 7). The hot sub-relations, on the other hand, undergo the special treatment in Lines 8 and 9.

Algorithm 6 *treeJoin*(\mathcal{R}, \mathcal{S})

Input: Two relations to be joined.

Output: The join results.

```

Constant:  $|\kappa_{\mathcal{R}}|_{max}$  and  $|\kappa_{\mathcal{S}}|_{max}$ ,
the number of hot keys to be collected
from  $\mathcal{R}$  and  $\mathcal{S}$ , respectively.
1:  $\kappa_{\mathcal{R}} = \text{getHotKeys}(\mathcal{R}, |\kappa_{\mathcal{R}}|_{max})$ 
2:  $\kappa_{\mathcal{S}} = \text{getHotKeys}(\mathcal{S}, |\kappa_{\mathcal{S}}|_{max})$ 
3:  $\kappa_{\mathcal{RS}} = \kappa_{\mathcal{R}} \text{.join}(\kappa_{\mathcal{S}})$ 
4: broadcast  $\kappa_{\mathcal{RS}}$  to all executors
5:  $\langle \mathcal{R}_H, \mathcal{R}_C \rangle =$ 
    $\text{splitPartitionsLocally}(\mathcal{R}, \text{rec} \rightarrow \text{key}_{\text{rec}} \in \kappa_{\mathcal{RS}}.\text{keys})$ 
6:  $\langle \mathcal{S}_H, \mathcal{S}_C \rangle =$ 
    $\text{splitPartitionsLocally}(\mathcal{S}, \text{rec} \rightarrow \text{key}_{\text{rec}} \in \kappa_{\mathcal{RS}}.\text{keys})$ 
7:  $\text{joined\_index}_C = \text{buildJoinedIndex}(\mathcal{R}_C, \mathcal{S}_C)$ 
8:  $\text{unraveled}_{\mathcal{R}_H} = \mathcal{R}_H.\text{map}(\text{rec} \rightarrow \text{map}_{\text{unravel}}(\text{rec}, \text{swap} = \text{false}))$ 
9:  $\text{unraveled}_{\mathcal{S}_H} = \mathcal{S}_H.\text{map}(\text{rec} \rightarrow \text{map}_{\text{unravel}}(\text{rec}, \text{swap} = \text{true}))$ 
10:  $\text{joined\_index}_{AK} =$ 
    $\text{buildJoinedIndex}(\text{unraveled}_{\mathcal{R}_H}, \text{unraveled}_{\mathcal{S}_H})$ 
11:  $\text{joined\_index}_H = \text{joined\_index}_{AK}.\text{map}(\text{map}_{\text{stripKeyPadding}})$ 
12:  $\text{joined\_index} = \text{joined\_index}_H.\text{union}(\text{joined\_index}_C)$ 
13:  $\mathcal{Q} = \text{empty Dataset}$ 
14: while  $\text{joined\_index.nonEmpty}$  do
15:    $\langle \text{partial\_results}, \text{new\_index} \rangle =$ 
      $\text{treeJoinIteration}(\text{joined\_index})$ 
16:    $\mathcal{Q} = \mathcal{Q} \cup \text{partial\_results}$ 
17:    $\text{joined\_index} = \text{new\_index.randomShuffle}$ 
18: end while
Return  $\mathcal{Q}$ 

```

The special treatment (formalized in Alg. 7) avoids collecting all the records of a hot key on one executor, and replaces the splitting of the joined lists of the hot key with local processing performed on the individual executors. Each partition of \mathcal{R} and \mathcal{S} is used to locally produce keyed records that when grouped by their keys, produce output that mimics the output of the first *treeJoinIteration*. Hence, the load imbalance of the first *treeJoinIteration* is evaded.

We only discuss \mathcal{R} , but the logic applies to \mathcal{S} . For every record, rec_i , in \mathcal{R} , its key, $\text{key}_{\text{rec}_i}$, is extracted (Line 2 in Alg. 7), and δ_1 and δ_2 , the number of sub-lists from \mathcal{R} and \mathcal{S} , respectively, are computed (Lines 3 - 9) based on Eqn. 1. If the initial joined index was to be built as explained in *treeJoinBasic* (Line 1 in Alg. 1), the two lists of that key would have been chunked into these many sub-lists during the splitting of the initial joined index (Line 4 in Alg. 3). That is, each of the δ_1 sub-lists of the first list would have been produced with each of the δ_2 sub-lists of the second list (Line 5 in Alg. 3). Knowing these numbers of sub-lists allows the executors to mimic this process without grouping the records of any hot key in a single partition. Each executor

⁵Quantifying $|\kappa_{\mathcal{R}}|_{max}$ and $|\kappa_{\mathcal{S}}|_{max}$ based on multiple parameters pertaining to the datasets and the hardware is discussed in § 7.

produces rec_i δ_2 times keyed by an *augmented key*. The augmented key has the original key, and two sub-list ids: a sub-list id from the δ_1 sub-lists and another from the δ_2 sub-lists. The first sub-list id of the augmented key is randomly chosen from the δ_1 sub-lists (Line 10 in Alg. 7). The second sub-list id assumes all the possible values from the δ_2 sub-lists (Lines 11 - 17 in Alg. 7). When processing a record from \mathcal{S} , the sub-list ids in its augmented keys are swapped, as per the different *swap* values in Lines 8 and 9 in Alg. 6.

Algorithm 7 $map_{unravel}(rec_i, swap)$

Local: $\kappa_{\mathcal{RS}}$, a map from the hot keys to the frequencies of the keys in the relation and in the other relation,
Input: A record with a hot key from a relation, and a flag to swap the frequencies and the sub-list ids.
Output: the unraveled records of rec_i .
Assumes: The key of rec_i exists in $\kappa_{\mathcal{RS}}$.
1: $u = \text{empty Buffer}$
2: $key_{rec_i} = \text{getKey}(rec_i)$
3: **if** $swap$ **then**
4: $(\ell_2, \ell_1) = \kappa_{\mathcal{RS}}[key_{rec_i}]$
5: **else**
6: $(\ell_1, \ell_2) = \kappa_{\mathcal{RS}}[key_{rec_i}]$
7: **end if**
8: $\delta_1 = \lceil \sqrt[3]{\ell_1} \rceil$
9: $\delta_2 = \lceil \sqrt[3]{\ell_2} \rceil$
10: $sub_list_id_1 = \text{getRandom}(\{0, \dots, \delta_1 - 1\})$
11: **for all** $sub_list_id_2 \in \{0, \dots, \delta_2 - 1\}$ **do**
12: **if** $swap$ **then**
13: $key' = \langle key_{rec_i}, sub_list_id_2, sub_list_id_1 \rangle$
14: **else**
15: $key' = \langle key_{rec_i}, sub_list_id_1, sub_list_id_2 \rangle$
16: **end if**
17: $u.append(\langle key', rec_i \rangle)$
18: **end for**
Return u

The unraveled forms of \mathcal{R}_H and \mathcal{S}_H produced by Alg. 7 (Lines 8 and 9 in Alg. 6) have augmented keys, and are used to build a joined index, $joined_index_{AK}$, based on these augmented keys. For each original hot key in $\kappa_{\mathcal{RS}}$, each record in \mathcal{R} is matched with every sub-list in \mathcal{S} . However, because this matching is done using $\delta_1 \times \delta_2$ augmented keys, the matching does not hot-spot on a single index partition, but is rather load-balanced between the $joined_index_{AK}$ partitions. $joined_index_{AK}$ mimics the hot-key entries of the index produced by the first *treeJoinIteration* of *treeJoinBasic*. The only difference is that $joined_index_{AK}$ contains augmented keys. These augmented keys are stripped back to the original keys using $map_{stripKeyPadding}$ (Line 11 in Alg. 6). Then, the resulting $joined_index_H$ of the hot keys is unioned with the cold $joined_index_C$ (Line 12 in Alg. 6), and the *treeJoin* algorithm proceeds exactly like *treeJoinBasic*.

$map_{stripKeyPadding}$:

$$\langle \langle key, sub_list_id_1, sub_list_id_2 \rangle, \mathcal{L}_1, \mathcal{L}_2 \rangle \rightarrow \langle key, \mathcal{L}_1, \mathcal{L}_2 \rangle$$

Notice that load balancing based on augmented-keys assumes the records of the hot keys are randomly distributed among the input partitions of \mathcal{R} and \mathcal{S} . If this is not the case, the records of the hot keys can be migrated and balanced among the input partitions. Detecting high variance in the hot key frequencies across partitions can be done while merging their frequencies in a tree-like manner. A similar approach has been employed in [60, 61] to minimize the communication cost in Track-Join, a PRPD-like algorithm.

Fig. 3 shows an example of building the initial joined index when joining the \mathcal{R} and \mathcal{S} given in Fig. 2 using *treeJoinBasic*

(Alg. 1) and of *treeJoin* (Alg. 6). The example assumes each dataset has 6 partitions, with the partition number shown as a subscript. Fig. 3(a) shows the partitions of the input relations. Fig. 3(b) shows the partitions of the initial index, $joined_index_0$ produced by *treeJoinBasic*. Fig. 3(c) through Fig. 3(f) show the processing steps of *treeJoin*. Fig. 3(c) shows $\kappa_{\mathcal{RS}}$, the hot-keys map broadcasted to all executors. Its keys are 1 and 2, and its values are tuples of their frequencies in \mathcal{R} and \mathcal{S} , respectively. Based on Eqn. 1, each list of records for keys 1 and 2 will be broken into two sub-lists. \mathcal{R}_C and \mathcal{S}_C are not shown for brevity, but the partitions of the initial cold joined index produced by them is shown in Fig. 3(d). Fig. 3(e) shows the partitions of $unraveled_{\mathcal{R}_H}$ and $unraveled_{\mathcal{S}_H}$, with the randomly generated sub-list ids underlined. $unraveled_{\mathcal{R}_H}$ and $unraveled_{\mathcal{S}_H}$ are used to produce $joined_index_{AK}$, whose partitions are shown in Fig. 3(f).

Fig. 3 helps contrasting the load balancing of *treeJoinBasic* and *treeJoin*. In the case of *treeJoinBasic*, the partition with the heaviest load, $joined_index_{00}$, produces 20 pairs of records, while that with the lightest load, $joined_index_{04}$ and $joined_index_{05}$, produces 0 pairs of records. In the case of *treeJoin*, we assume each partition of the initial cold joined index is unioned with the corresponding partition of the initial hot joined index, produced by stripping the keys of $joined_index_{AK}$ in Fig. 3(f). The partition with the heaviest load, $joined_index_{05}$, produces 10 pairs of records, while that with the lightest load, $joined_index_{02}$ and $joined_index_{03}$, produces 4 pairs of records.

4.4 Executing Same-Attribute Self-Joins

While Tree-Join can execute self-joins in the same way it handles normal equi-joins, there are special optimizations that can be introduced in that case. We discuss an optimization that results in reducing the processing and IO by roughly half.

Because we are processing a single relation, this relation is split into its cold and hot sub-relations. Hence, in Alg. 6, Lines 2 6, and 9 are omitted, and $\kappa_{\mathcal{RS}} = \kappa_{\mathcal{R}}$. In Line 7, instead of building a cold joined index, where each key in the index has two joined lists of records, a cold index is built, where each key has a single list of records. The join results of a cold key in the cold index are produced by outputting the key with all pairs of records where the first record is before the second in the record list. This corresponds to producing the upper triangle in a matrix whose rows and columns represent the records of the key, and each cell represents the pair of corresponding records.

For a hot key that has a long list of records, the unravelling (Line 8) happens in a way simpler than Alg. 7 since there is no *swap* parameter. The sub-list ids are picked from the range $[0, \dots, \delta - 1]$, where $\delta = \lceil \sqrt[3]{\ell} \rceil$, and ℓ is the length of the records in the list of this key. To realize the processing and IO savings, In Lines 12 - 17 in Alg. 7, a record with an augmented key $\langle key, sub_list_id_1, sub_list_id_2 \rangle$ is only output if $sub_list_id_1 \leq sub_list_id_2$. Otherwise, it is output with the reversed augmented key, $\langle key, sub_list_id_2, sub_list_id_1 \rangle$.

4.5 Defining Hot Keys

From the key-independence observation, keys can be considered in isolation. If the joined lists are not chunked, the time to produce the join results on 1 executor using Shuffle-Join is $\Delta_{ShuffleJoin} \approx \Theta(\ell^2)$. Meanwhile, the end-to-end

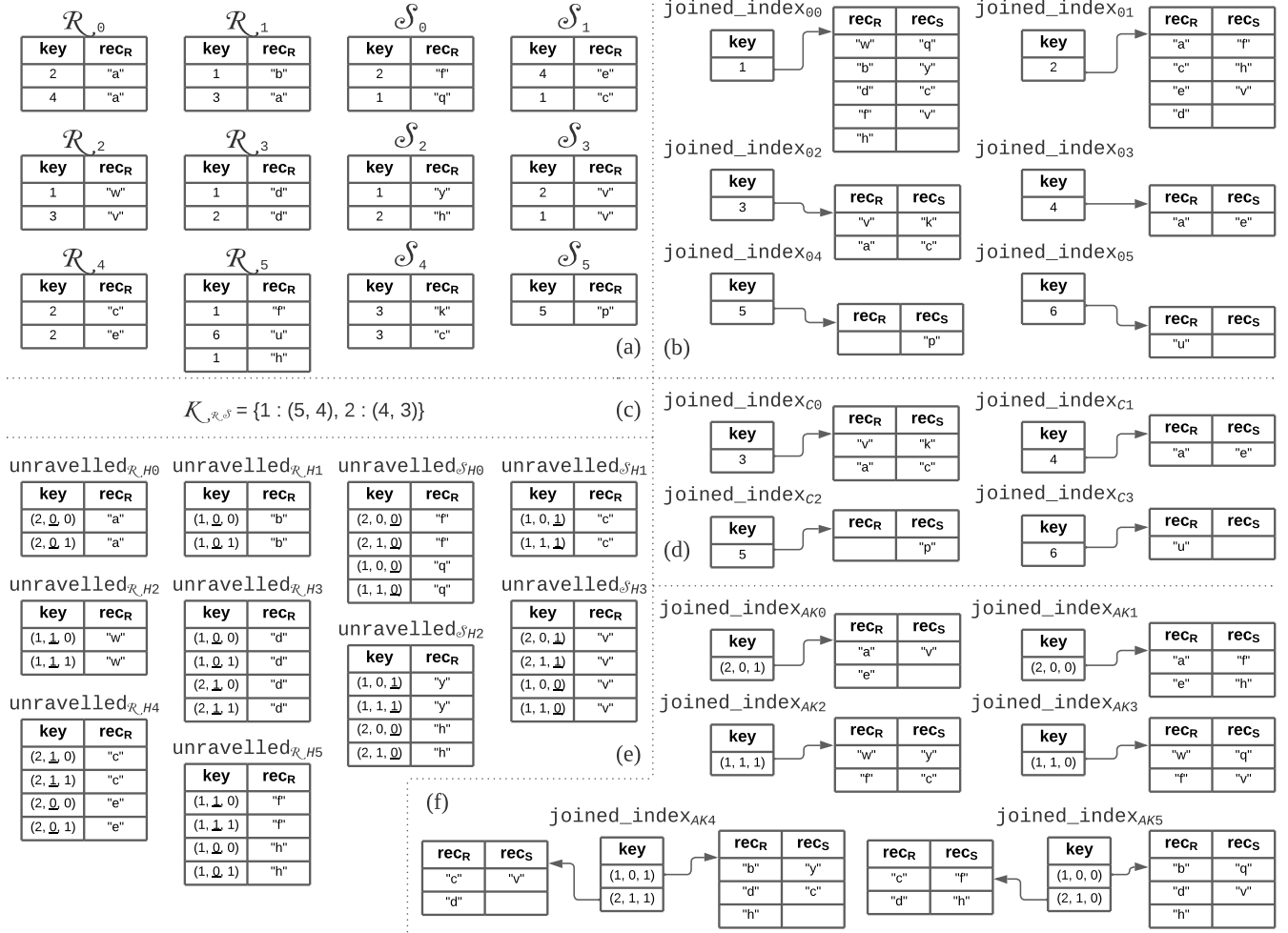


Figure 3: An example showing the difference in load balancing in the first iteration between *treeJoinBasic* and *treeJoin* when joining the \mathcal{R} and \mathcal{S} given in Fig. 2. The example assumes each dataset has 6 partitions. (a) The partitions of the input relations. (b) The partitions of the initial index, $joined_index_0$, built from the input relations in (a) using *treeJoinBasic*. (c) through (f) show the processing steps of *treeJoin*. (c) The $\kappa_{\mathcal{R},\mathcal{S}}$ broadcasted to all executors containing the hot-keys and their frequencies in \mathcal{R} and \mathcal{S} . (d) The partitions of the cold joined index. (e) The partitions of $unraveled_{\mathcal{R}_H}$ and $unraveled_{\mathcal{S}_H}$. (f) The partitions of $joined_index_{AK}$ built using $unraveled_{\mathcal{R}_H}$ and $unraveled_{\mathcal{S}_H}$.

Tree-Join processing time, $\Delta_{treeJoin}$, is the time taken to chunk the joined lists, the time to randomly shuffle the pairs of sub-lists over the network, and the time taken by the $\left\lceil \ell^{\frac{2}{3}} \right\rceil$ subsequent executors in the next iteration. A key is considered hot and is worth chunking if $\Delta_{ShuffleJoin} > \Delta_{treeJoin}$ using the worst-case scenario for Tree-Join, i.e., a single stage and exactly one splitter. Given n available executors, this condition is expressed in Rel. 2.

$$\ell^2 > \left((1 + \lambda) + \left\lceil \frac{\ell^{\frac{2}{3}}}{n} \right\rceil \right) \times \ell^{\frac{4}{3}} \quad (2)$$

The ceiling can be relaxed while preserving the correctness of Ineq. 2. One (non-tight) value for ℓ that provably satisfies Ineq. 2 for any $\lambda > 0$ and any $n > 1$ is $(1 + \lambda)^{\frac{3}{2}}$. This value is used in the rest of the paper to define the minimum frequency for a key to be hot.

Algorithm 8 *isHotKey*($\langle key, \mathcal{L}_1, \mathcal{L}_2 \rangle$)

Input: A tuple of the key, and two joined lists of records.

Output: Whether the joined lists should be chunked.

Constant: λ the ratio of network to disk costs.

1: $\ell_1 = |\mathcal{L}_1|$ // The length of \mathcal{L}_1 .

2: $\ell_2 = |\mathcal{L}_2|$ // The length of \mathcal{L}_2 .

3: $\ell = \sqrt{\ell_1 \times \ell_2}$ // The effective length if $\ell_1 = \ell_2$.

Return $\ell > (1 + \lambda)^{\frac{3}{2}}$

4.6 The Number of Iterations

Since the overhead of allocating the executors for a stage was ignored, we make the case the number of iterations in this multistage join is very small.

From the key-independence observation, the join is concluded when the results for the last key are computed. Assuming all other factors are equal, the last key to compute has the longest pair of joined lists, ℓ_{max} . After the first stage, each of the subsequent executors of the next iteration

inherits a pair of lists whose lengths are $\ell_{max}^{\frac{2}{3}}$. This chunking continues for t times as long as the lengths exceed $(1 + \lambda)^{\frac{2}{3}}$. Hence, the following inequality holds for t .

$$(1 + \lambda)^{\frac{2}{3}} < \underbrace{\ell_{max}^{\frac{2}{3}} \cdot \ell_{max}^{\frac{2}{3}} \cdots \ell_{max}^{\frac{2}{3}}}_{t \text{ times}}$$

Hence, $(1 + \lambda)^{\frac{2}{3}} < \ell_{max}^{\frac{2}{3}t}$. Raising both sides to the $(\frac{3}{2})^t$ power yields $(1 + \lambda)^{\frac{3}{2}t} < \ell_{max}^t$. Taking the log with base $1 + \lambda$ on both sides yields the following.

$$\left(\frac{3}{2}\right)^{t+1} < \log_{1+\lambda}(\ell_{max})$$

Taking the log with base $\frac{3}{2}$ yields Rel. 3.

$$t < \log_{\frac{3}{2}}(\log_{1+\lambda}(\ell_{max})) - 1 \quad (3)$$

From Ineq. 3, the number of iterations is $O(\log(\log(\ell_{max})))$, which grows very slowly with ℓ_{max} .

5. THE SMALL-LARGE OUTER-JOINS

The scenario of Small-Large outer-joins arise when $\mathcal{R} \gg \mathcal{S}$ and \mathcal{S} can be assumed to fit in the memory of each executor. An index can be built for the small relation, \mathcal{S} , the driver collects the index locally, and broadcasts it to all n executors performing the join. Broadcasting \mathcal{S} can be done in time that is logarithmic in n [11, 67], and can hence be faster than shuffling the large relation, \mathcal{R} , across the network.

mapbuildIndex:
 $rec_i \rightarrow \langle key_{rec_i}, rec_i \rangle$

Algorithm 9 *indexBroadcastJoin*(\mathcal{R}, \mathcal{S})

Input: Two relations to be joined.
Output: The join results.
Assumes: \mathcal{S} fits in memory. $\mathcal{R} \gg \mathcal{S}$.
1: $index = \mathcal{S}.map(mapbuildIndex).groupByKey$
2: broadcast $index$ to all executors
3: $\mathcal{Q} = \mathcal{R}.map(mapindexBroadcastJoin)$
Return \mathcal{Q}

Alg. 9 broadcasts the index instead of \mathcal{S} , and hence the algorithm family name, Index-Broadcast-Join. Assuming each executor, e_i , can accommodate the index of \mathcal{S} in memory. For each record in its local partition, \mathcal{R}_i , the executor extracts the key, probes the local index of \mathcal{S} with that key, and produces the join results. The local join is shown in Alg. 10.

Algorithm 10 *mapindexBroadcastJoin*(rec_i)

Local: $index$, a map from each key in the replicated relation to all the records with that key.
Input: A record from the non-replicated relation.
Output: A list of triplets representing the join of rec_i with $index$.
1: $u = \text{empty Buffer}$
2: $key_{rec_i} = getKey(rec_i)$
3: **for all** $rec_j \in index[key_{rec_i}]$ **do**
4: $u.append(\langle key_{rec_i}, rec_i, rec_j \rangle)$
5: **end for**
Return u

AM-Join utilizes Broadcast-Joins for keys that are hot in only one relation. Extending AM-Join to outer-joins entails performing Small-Large outer-joins. We extend Index-Broadcast-Join (IB-Join) to outer-joins for the best performance of AM-Join outer-joins. The Index-Broadcast-Full-Outer-Join (IB-FO-Join) algorithm is in Alg. 11. The left-outer-join and the right-outer-join are mere simplifications.

Like the inner-join, IB-FO-Join builds an index on the small relation, collects it at the driver, and broadcasts it to all the executors. The results of the left-outer-join are then computed. The *mapbroadcastLeftOuterJoin* function (Alg. 12) is similar to Alg. 10, but also produces *unjoined* records from the non-replicated relation.

To produce the full-outer-join, IB-FO-Join needs to also produce the right-anti join results, i.e., the *unjoinable* records in the small replicated relation. The driver finds the unjoinable keys in the replicated relation by utilizing the already replicated relation. The *mapgetRightJoinableKey* (Alg. 13) produces a set for each record in the large non-replicated relation. The set either has a single key from the replicated relation if the key is joinable with the non-replicated relation, or is empty otherwise. The driver then unions these sets, first on each executor, and then across the network. The union constitutes the set of joined keys in the replicated relation. The index keys not in this union constitute the unjoinable keys.

Algorithm 11 *indexBroadcastFullOuterJoin*(\mathcal{R}, \mathcal{S})

Input: Two relations to be joined.
Output: The join results.
Assumes: \mathcal{S} fits in memory. $\mathcal{R} \gg \mathcal{S}$.
1: $index = \mathcal{S}.map(mapbuildIndex).groupByKey$
2: broadcast $index$ to all executors
3: $\mathcal{Q}_{leftOuter} = \mathcal{R}.map(mapbroadcastLeftOuterJoin)$
4: $keys_{joined} = \mathcal{R}$
5: $.map(mapgetRightJoinableKey)$
6: $.combine(unionSets)$
7: $.treeAggregate(unionSets)$
8: $keys_{unjoinable} = index.keys - keys_{joined}$
9: broadcast $keys_{unjoinable}$ to all executors
10: $\mathcal{Q}_{rightAnti} = \mathcal{S}.map(mapRightAntiJoin)$
Return $\mathcal{Q}_{leftOuter} \cup \mathcal{Q}_{rightAnti}$

Algorithm 12 *mapbroadcastLeftOuterJoin*(rec_i)

Local: $index$, a map from each key in the replicated relation to all the records with that key.
Input: A record from the non-replicated relation.
Output: A list of triplets representing the left-outer-join of rec_i with $index$.
1: $u = \text{empty Buffer}$
2: $key_{rec_i} = getKey(rec_i)$
3: **if** key_{rec_i} in $index$ **then**
4: **for all** $rec_j \in index[key_{rec_i}]$ **do**
5: $u.append(\langle key_{rec_i}, rec_i, rec_j \rangle)$
6: **end for**
7: **else**
8: $u.append(\langle key_{rec_i}, rec_i, null \rangle)$
9: **end if**
Return u

The driver then broadcasts these unjoinable keys back to the executors, and maps the original small relation using *mapRightAntiJoin* (Alg. 14). Each executor scans its local partition of the small relation, and outputs only the records whose keys are unjoinable. The left-outer-join results are unioned with the right-anti join results to produce the full-outer-join results.

Algorithm 13 *map_{getRightJoinableKey}(*rec_i*)*

Local: *index*, a map from each key in the replicated relation to all the records with that key.

Input: A record from the non-replicated relation.

Output: The key of *rec_i* if it is joinable with *index*.

```
1: u = empty Set
2: keyreci = getKey(reci)
3: if keyreci ∈ index.keys then
4:   u.append(keyreci)
5: end if
Return u
```

5.1 Optimizations

IB-FO-Join can be optimized as follows.

1. The driver should send the joinable keys over the network if they are fewer than the unjoinable keys (Line 9 of Alg. 11). In that case, the condition in Line 2 of Alg. 14 has to be reversed.
2. Lines 3 and 5 in Alg. 11 can be combined into a single *mapRec* function to reduce the number of scans on the large relation.
3. In a shared-nothing architecture where an executor, *e_i*, can scan its data partition, Lines 5 and 6 in Alg. 11 can be combined. A single set can be allocated and populated as *R_i* is scanned.
4. In a shared-nothing architecture that supports both multicasting and broadcasting, instead of broadcasting the index to all the executors (Line 2 in Alg. 9 and Alg. 11), the driver may broadcast the unique keys only. Instead of the local joins (Line 3 in Alg. 9 and Alg. 11), each executor, *e_i*, joins the *S* keys with its *R_i* and sends the joinable keys to the driver. The driver multicasts each *S* record only to the executors that have its joinable partitions. Each *e_i* joins the received records with its *R_i*. The driver need not compute the unjoinable *S* keys (Lines 4–8 in Alg. 11), since they are the keys not multicasted at all.

Algorithm 14 *map_{rightAntiJoin}(*rec_j*)*

Local: *keys_{unjoinable}*, a set of unjoinable keys.

Input: A record from the replicated relation.

Output: The join results of *rec_j* if its key is in *keys_{unjoinable}*.

```
1: keyrecj = getKey(recj)
2: if keyrecj ∈ keysunjoinable then
  Return <keyrecj, null, recj>
3: end if
```

5.2 Comparison with the State-of-the-Art Algorithms

A main difference between the proposed IB-FO-Join (Alg. 11), DER [78] and DDR [24] is subtle but effective. To flag the unjoined records in the *n* executors, IB-FO-Join utilizes the unique keys, instead of the DBMS-assigned record ids in case of DER⁶ or entire records in case of DDR. Assuming the key is of the same size as the record id, and is significantly smaller than the record, sending unique keys reduces the network load, and scales better with a skewed *S*.

The other major difference is how the unjoinable records are identified after the first Broadcast-Join. DER hashes the

⁶A minor advantage of the IB-Join family is abolishing the dependency on DBMS-specific functionality. This facilitates its adoption in any shared-nothing architecture.

unjoined ids from all executors over the network, and performs an inner Hash-Join. This entails hashing the records of *R*, each of size *m_R*, and the unjoinable ids of *S*, each of size *m_{id}* over the network. The communication cost of this step is $(n + 1) \times |S| \times m_{id} + |R| \times m_R$. DDR hashes the *S* records, each of size *m_S*, from all executors, incurring a communication cost of $n \times |S| \times m_S$, which is as costly as the first Broadcast-Join itself. IB-FO-Join collects and broadcasts the unique keys, each of size *m_b* (Lines 4 – 7 and 9 of Alg. 11, respectively), with a communication cost of $2n \times |S| \times m_b$. This is much more efficient than DER and DDR, even without considering that broadcasting the unique keys is done in time logarithmic in *n*.

6. THE AM-JOIN ALGORITHM

AM-Join employs the Tree-Join and the Broadcast-Joins (we utilize Index-Broadcast-Join for its communication efficiency) to maximize the executors' utilization, and minimize the communication cost. AM-Join starts by collecting a map from hot keys to their frequencies for both relations, *κ_R* and *κ_S*. Then, it splits each relation into four sub-relations containing the keys that are hot in both sides, the keys that are hot in its side but cold in the other side, the keys that are hot in the other side but cold in its side, and the keys that are cold in both sides, respectively (§ 6.1). Therefore, *R* is split into *R_{HH}*, *R_{HC}*, *R_{CH}* and *R_{CC}*, and *S* is split similarly into *S_{HH}*, *S_{HC}*, *S_{CH}* and *S_{CC}*. Irrespective of the keys in *κ_R* and *κ_S*, it is provable that the join results are the union of the four joins in Eqn. 4.

Algorithm 15 *amJoin(R, S)*

Input: Two relations to be joined.

Output: The join results.

Constant: $|\kappa_R|_{max}$ and $|\kappa_S|_{max}$,
the number of hot keys to be collected
from *R* and *S*, respectively.

```
1: κR = getHotKeys(R, |κR|max)
2: κS = getHotKeys(S, |κS|max)
3: <RHH, RHC, RCH, RCC> = splitRelation(R, κR, κS)
4: <SHH, SHC, SCH, SCC> = splitRelation(S, κS, κR)
5: Q = treeJoin(RHH, SHH)
6:   ∪ indexBroadcastJoin(RHC, SCH)
7:   ∪ indexBroadcastJoin(SHC, RCH)
   .map(mapswapJoinedRecords)
8:   ∪ shuffleJoin(RCC, SCC)
Return Q
```

For the example of the two relations in Fig. 1(a), assuming the hot keys on either *R* and *S* are those occurring multiple times, then *κ_R* and *κ_S* are the maps {1 : 2, 2 : 2, 3 : 2, 4 : 2} and {1 : 2, 6 : 2, 11 : 2, 12 : 2}, respectively. Fig. 4(b) shows the sub-relations of *R* and *S* paired together to be joined, according to Eqn. 4. If all the joins in Eqn. 4 are inner-joins, then the inner-join results of *R* and *S* are given in Fig. 1(b).

$$\begin{aligned} Q = & R_{HH} \bowtie S_{HH} \\ & \cup R_{HC} \bowtie S_{CH} \\ & \cup R_{CH} \bowtie S_{HC} \\ & \cup R_{CC} \bowtie S_{CC} \end{aligned} \quad (4)$$

Since the first join involves keys that are hot in both the joined relations, Tree-Join (Alg. 6) is used. For the second and the third joins in Eqn. 4, the cold side is likely to have few keys, since they are a subset of the hot keys on the other side of the join, each with few records. Hence, these two joins

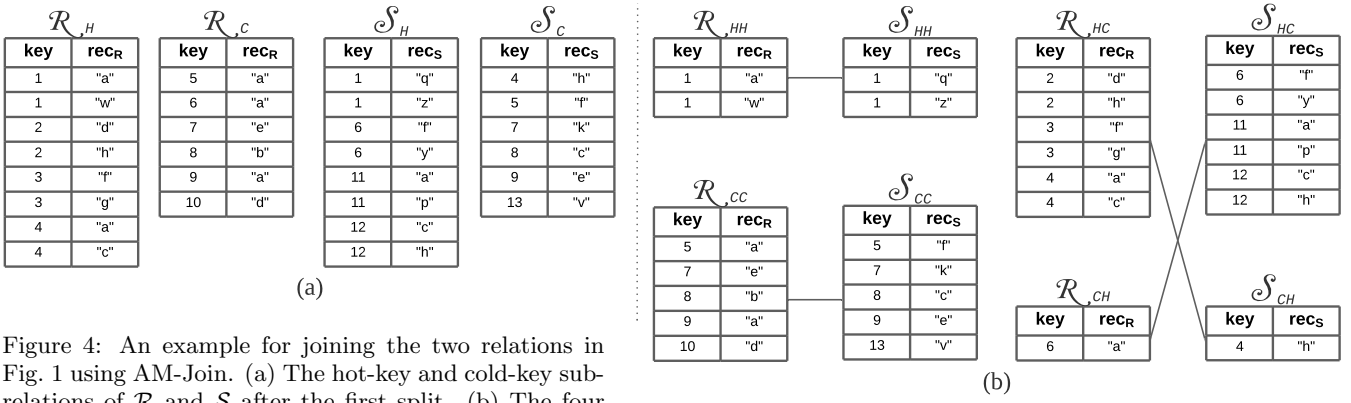


Figure 4: An example for joining the two relations in Fig. 1 using AM-Join. (a) The hot-key and cold-key sub-relations of \mathcal{R} and \mathcal{S} after the first split. (b) The four sub-relations for each of the two input relations after the second split, and their joins based on Eqn. 4.

are considered Small-Large joins. Each record resulting from the third join is swapped so the a attributes from \mathcal{R} precede the c attributes from \mathcal{S} , where a and c are their non-join attribute(s), respectively. Finally, the fourth join involves keys that are hot on neither side, and is hence performed using a Shuffle-Join. The algorithm is shown in Alg. 15. One optimization is passing the hot key maps, $\kappa_{\mathcal{R}}$ and $\kappa_{\mathcal{S}}$, to Tree-Join instead of double-computing them.

Notice that in the case of processing same-attribute self-joins, the hot keys are identical on both sides of the join. Hence, the second and the third Small-Large joins produce no results. In that case, AM-Join reduces to Tree-Join.

While the AM-Join algorithm bears some resemblance to the PRPD family, it deviates in a core aspect. PRPD assigns a key as hot to the relation that has more records for that key. AM-Join independently collects the hot keys for \mathcal{R} and \mathcal{S} , resulting in the simple and elegant Eqn. 4. Eqn. 4 leads to (a) AM-Join utilizing the scalable Tree-Join to join the keys that are hot in both \mathcal{R} and \mathcal{S} , and (b) extending AM-Join smoothly to all outer-join variants (§ 6.3).

6.1 Splitting the Relations

Once the hot keys for both \mathcal{R} and \mathcal{S} are collected, each relation is split into its four sub-relations. We only discuss \mathcal{R} , but the logic applies to \mathcal{S} . This *splitRelation* module (Alg. 16) proceeds in two rounds. It first splits \mathcal{R} into \mathcal{R}_H , the sub-relation whose keys are in $\kappa_{\mathcal{R}}$, and \mathcal{R}_C , the cold-key records in \mathcal{R} . In the example in Fig. 1, the results of the first-round of splitting is in Fig. 4(a). In the second round, \mathcal{R}_H is split into \mathcal{R}_{HH} , the sub-relation whose keys are in $\kappa_{\mathcal{S}}$, and \mathcal{R}_{HC} , the remaining records in \mathcal{R}_H . \mathcal{R}_C is similarly split using $\kappa_{\mathcal{S}}$ into \mathcal{R}_{CH} and \mathcal{R}_{CC} . In the example in Fig. 1, the second-round of splitting are in Fig. 4(b).

Algorithm 16 *splitRelation*($\mathcal{R}, \kappa_{\mathcal{R}}, \kappa_{\mathcal{S}}$)

Input: A relation to be split,
its hot keys map,
and the hot keys map of the other relation.

Output: The four splits of \mathcal{R} .

```

1:  $\langle \mathcal{R}_H, \mathcal{R}_C \rangle =$ 
    $\text{splitPartitionsLocally}(\mathcal{R}, \text{rec} \rightarrow \text{key}_{\text{rec}} \in \kappa_{\mathcal{R}}.\text{keys})$ 
2:  $\langle \mathcal{R}_{HH}, \mathcal{R}_{HC} \rangle =$ 
    $\text{splitPartitionsLocally}(\mathcal{R}_H, \text{rec} \rightarrow \text{key}_{\text{rec}} \in \kappa_{\mathcal{S}}.\text{keys})$ 
3:  $\langle \mathcal{R}_{CH}, \mathcal{R}_{CC} \rangle =$ 
    $\text{splitPartitionsLocally}(\mathcal{R}_C, \text{rec} \rightarrow \text{key}_{\text{rec}} \in \kappa_{\mathcal{S}}.\text{keys})$ 
Return  $\langle \mathcal{R}_{HH}, \mathcal{R}_{HC}, \mathcal{R}_{CH}, \mathcal{R}_{CC} \rangle$ 

```

The splitting is done by each executor reading its local partition sequentially, checking if the record key exists in the hot-key set, and writing it to either the hot-key sub-relation or the cold-key sub-relation. The splitting involves no communication between the executors. The two rounds can be optimized into one.

6.2 When not to Perform Broadcast-Joins?

The second and third joins in Eqn. 4 are executed using Broadcast-Joins. We only discuss the second join, but the logic applies to the third. For the Broadcast-Join assumption to hold, broadcasting the records of the small relation, \mathcal{S}_{CH} , over the network has to be faster than splitting the large relation, \mathcal{R}_{HC} , among the n executors over the network. From [11], the time to read \mathcal{S}_{CH} and broadcast it follows the Big- Θ below.

$$\Delta_{\text{broadcast}_{\mathcal{S}_{CH}}} \approx \Theta(|\mathcal{S}_{CH}| \times m_{\mathcal{S}} \times (1 + \lambda \times \log_{\lambda+1}(n)))$$

Let $m_{\mathcal{R}}$ be the average size of a record in \mathcal{R} . The time to read \mathcal{R}_{HC} and split it among the n executors follows the Big- Θ below.

$$\Delta_{\text{split}_{\mathcal{R}_{HC}}} \approx \Theta(|\mathcal{R}_{HC}| \times m_{\mathcal{R}} \times (1 + \lambda))$$

At the time of executing the second join in Eqn. 4, \mathcal{R}_{HC} and \mathcal{S}_{CH} have already been computed. A Broadcast-Join is performed if $\Delta_{\text{split}_{\mathcal{R}_{HC}}} \geq \Delta_{\text{broadcast}_{\mathcal{S}_{CH}}}$. Otherwise, Shuffle-Join is performed.

6.3 The Outer Variants of AM-Join

Due to the AM-Join elegant design, the outer-join variants are minor modifications of the inner-join in Alg. 15. The only difference is that some of the four joins of Eqn. 4 are executed using outer-join algorithms. Table. 2 shows the algorithm used for each of the four joins to achieve the outer-join variants of AM-Join. The first and the fourth joins are performed using Tree-Join and a Shuffle outer-join, respectively. The second and third joins are performed using a Broadcast-Join or its left-outer variant (we utilize Index-Broadcast-Join or Index-Broadcast-Left-Outer-Join for their communication efficiency). Applying the outer-joins in Table. 2 to the joins in Fig. 4(b) yields the left-outer, right-outer, and full-outer-join results in Fig. 1(c), Fig. 1(d), and Fig. 1(e), respectively.

	left-outer AM-Join	right-outer AM-Join	full-outer AM-Join
$\mathcal{R}_{HH} \bowtie \mathcal{S}_{HH}$	Tree-Join	Tree-Join	Tree-Join
$\mathcal{R}_{HC} \bowtie \mathcal{S}_{CH}$	Index-Broadcast-Left-Outer-Join	Index-Broadcast-Join	Index-Broadcast-Left-Outer-Join
$\mathcal{S}_{HC} \bowtie \mathcal{R}_{CH}$	Index-Broadcast-Join	Index-Broadcast-Left-Outer-Join	Index-Broadcast-Left-Outer-Join
$\mathcal{R}_{CC} \bowtie \mathcal{S}_{CC}$	Shuffle left-outer-join	Shuffle right-outer-join	Shuffle full-outer-join

Table 2: The algorithms for the four sub-joins of Eqn. 4 of the outer variants of AM-Join.

Unlike the state-of-the-art distributed industry-scale algorithms, the different flavors of SkewJoin [19] built on top of Microsoft SCOPE, AM-Join supports all variants of outer-joins without record deduplication or custom partitioning of the relations. Moreover, AM-Join does not require introducing a new outer-join operator variant that understands the semantics of *witness* tuples, a form of tuples introduced in [19] to extend SkewJoin to outer-joins.

7. COLLECTING HOT KEYS

Identifying hot keys in \mathcal{R} and \mathcal{S} is an integral part of Tree-Join and AM-Join, since it allows it allows for load-balancing the executors (§ 4.3), and for splitting the joined relations into the sub-relations going into Eqn. 4. The *getHotKeys* algorithm (Lines 1 and 2 in Alg. 6 and Lines 1 and 2 in Alg. 15) collects the hot keys for both \mathcal{R} and \mathcal{S} . The maximum numbers of hot keys collected for \mathcal{R} and \mathcal{S} are $|\kappa_{\mathcal{R}}|_{max}$ and $|\kappa_{\mathcal{S}}|_{max}$, respectively, are discussed in § 7.1. We only discuss $|\kappa_{\mathcal{R}}|_{max}$, but the logic applies to $|\kappa_{\mathcal{S}}|_{max}$. In § 7.2 we discuss the cost of collecting hot keys. We assume \mathcal{R} and \mathcal{S} are evenly distributed on the n executors and no record migration among the input partitions is necessary.

7.1 How many Hot Keys to Collect?

We only discuss $|\kappa_{\mathcal{R}}|_{max}$, but the logic applies to $|\kappa_{\mathcal{S}}|_{max}$. Any key with $(1 + \lambda)^{\frac{3}{2}}$ or more records is hot (Ineq. 2). Three upper bounds apply to $|\kappa_{\mathcal{R}}|_{max}$.

1. No more than $\frac{M}{m_b}$ hot keys can be collected, since no more keys of size m_b can fit in a memory of size M . The data structure overhead of the heavy-hitters algorithm is ignored for simplicity, but can be accounted for in the implementation.
2. The number of hot keys in \mathcal{R} cannot exceed $\frac{|\mathcal{R}|}{(1+\lambda)^{\frac{3}{2}}}$, from the Pigeonhole principle.
3. The second join in Eqn. 4 is executed using Broadcast-Join (e.g., Index-Broadcast-Join). Let $m_{\mathcal{S}}$ be the average record size in \mathcal{S} . \mathcal{S}_{CH} is computed after *getHotKeys*, but is bounded to fit in memory by Rel. 5.

$$|\mathcal{S}_{CH}| \leq \frac{M}{m_{\mathcal{S}}} \quad (5)$$

The keys in \mathcal{S}_{CH} are a subset of the keys in $\kappa_{\mathcal{R}}$. Each of these keys has frequency below $(1 + \lambda)^{\frac{3}{2}}$ in \mathcal{S}_{CH} . To ensure \mathcal{S}_{CH} fits in memory, we limit $|\kappa_{\mathcal{R}}|$ by Rel. 6.

$$|\kappa_{\mathcal{R}}|_{max} \leq \frac{|\mathcal{S}_{CH}|}{(1 + \lambda)^{\frac{3}{2}}} \quad (6)$$

Substituting Rel. 5 in Rel. 6 yields an upper bound on $|\kappa_{\mathcal{R}}|_{max}$.

Given the three upper bounds above, the maximum numbers of hot keys collected for \mathcal{R} , $|\kappa_{\mathcal{R}}|_{max}$, is given by Eqn. 7.

$$|\kappa_{\mathcal{R}}|_{max} = \min \left(\frac{\min \left(|\mathcal{R}|, \frac{M}{m_{\mathcal{S}}} \right)}{(1 + \lambda)^{\frac{3}{2}}}, \frac{M}{m_b} \right) \quad (7)$$

7.2 The Hot Keys Cost

The cost of collecting $|\kappa_{\mathcal{R}}|_{max}$ hot keys using the algorithm in [3] is the cost of scanning the local \mathcal{R}_i partitions in parallel, and the cost of merging the hot keys over the network in a tree-like manner. Given m_b and $m_{\mathcal{R}}$, the average sizes of a key and a \mathcal{R} record, respectively, the total cost is given by Rel. 8.

$$\Delta_{getHotKeys} = \frac{|\mathcal{R}| \times m_{\mathcal{R}}}{n} + |\kappa_{\mathcal{R}}|_{max} \times m_b \times \lambda \times \log(n) \quad (8)$$

We like to contrast collecting the hot keys using a distributed heavy-hitters algorithm to histogramming the relation using a distributed quantiles algorithm [57, 76, 36]. Assuming \mathcal{R} is distributed evenly between the n executors, and given an error rate, ϵ , the local heavy-hitters algorithm uses $\Theta(\frac{1}{\epsilon})$ space [54], while the local quantiles algorithm uses $O(\frac{1}{\epsilon} \log(\epsilon \frac{|\mathcal{R}|}{n}))$ space [29]⁷. Collecting heavy hitters is more precise given the same memory, and incurs less communication when merging the local statistics over the network to compute the global statistics.

8. EVALUATION RESULTS

We evaluated the scalability and the handling of skewed data of Tree-Join, Tree-Join-Basic, AM-Join, AM-Join-Basic (i.e., AM-Join using Tree-Join-Basic for joining keys that are hot on both sides of the join), Hash-Join, Broadcast-Join, Full-SkewJoin [19] (the state-of-the-art industry-scale algorithm of the PRPD family), and Fine-Grained partitioning for Skew Data (FGSD-Join) [36] (the state-of-the-art of the key-range-division family). We also evaluated the Spark v3.x joins⁸, the most advanced open-source shared-nothing algorithm. The two main optimizations of Spark3-Join are (a) dynamically changing the execution plan from Shuffle-Join to Broadcast-Join when one relation can fit in memory, and (b) dynamically combining and splitting data partitions to reach almost equi-size partitions for load balancing. Multicasting is not supported by Spark, the framework we used for evaluation. Evaluating multicasting algorithms (e.g., [61]) is left for future work.

The performance of the algorithms on outer-joins was in line with the inner-joins, reported below. However, we could

⁷This is the theoretical bound on any deterministic single-pass comparison-based quantiles algorithm, even if the algorithms in [57, 76, 36] do not necessarily use it.

⁸<https://databricks.com/blog/2020/05/29/adaptive-query-execution-speeding-up-spark-sql-at-runtime.html>, <https://docs.databricks.com/spark/latest/spark-sql/ae.html>

build the outer-join variants of neither Full-SkewJoin, since it depends on Microsoft SCOPE-specific deduplication, nor FGSD-Join, since it was missing in [36]. We compared the outer-join variant of the proposed IB-Join against DER [78] and DDR [24] on Small-Large outer-joins.

We conducted comprehensive experiments on reproducible synthetic realistic data, and on real proprietary data. All the experiments were executed on machines (driver and executors) with 8GB of memory, 20GB of disk space, and 1 core. Based on Ineq. 2 and Rel. 7, among the most popular 1000 keys, those that have 100 records or more were considered hot. These values agree with the guidelines of Full-SkewJoin. The sample for FGSD-Join was $10\times$ the number of partitions, and the number of partitions was $3\times$ to $5\times$ the number of executors.

The algorithms code and the code for the dataset generation and experiment running was written in Scala v2.11.12 and executed using Spark v2.4.3, except for the Spark v3.x experiments that were run on Spark v3.0.2. All the code was peer reviewed, and tested for correctness. The code will be available on <https://github.com/uber>.

8.1 Experiments on Synthetic Data

The synthetic data is a combination of random data generated using two processes. The first process generates a dataset of 10^9 records whose keys are uniformly selected from the positive range of the 32-bit Integer space. The second process generates a dataset with 10^7 records whose keys are drawn from a Zipf distribution with a skew-parameter α and a domain of 10^5 keys. The records of both processes have the same size, S .

Initially, the experiments were conducted using the Zipfian keys only. The Zipfian keys were generated using the Apache Commons math package, which uses the state-of-the-art inverse-CDF algorithm. Yet, generating skewed keys from a space of 10^5 was pushing the limits of the math package. The uniformly-distributed keys were eventually incorporated to increase the key space.

We refer to the combined dataset using the notation $D(\alpha, S)$. For instance, $D(0.5, 10^3)$ refers to a dataset whose records have a size of 10^3 Bytes, and has 10^9 records whose keys are uniformly selected from the positive Integer space, and 10^7 records whose keys are drawn from a Zipf-0.5 distribution with a range of 10^5 .

Two sizes of records were experimented with, $S = 10^2$, and $S = 10^3$ Bytes, representing relatively small and large records. The Zipf- α was varied between 0.0 and 1.0, representing uniform to moderately skewed data. Higher values of α are common in many applications⁹. However, higher values of α are expected to favor algorithms that handle data skew better, namely AM-Join(-Basic) and Tree-Join(-Basic). These four algorithms split the processing of each hot key among multiple executors. Finally, the number of executors used to execute the join was varied from 100 to 1000 executors to evaluate how the algorithms utilize more resources to scale to more skewed datasets. All algorithms were allowed 2 hours to execute each join.

8.1.1 Equi-Join Scalability with Data Skew

Fig. 5 shows the runtimes of the algorithms when joining two relations, each has records with a size of 10^2 Bytes, and has 10^9 records whose keys are uniformly selected from the

⁹One example is the word frequency in Wikipedia [77].

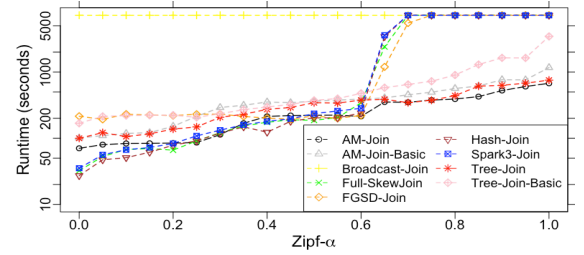


Figure 5: The runtime of the equi-join algorithms on 1000 executors for $D(\alpha, 100)$ while varying the Zipf- α .

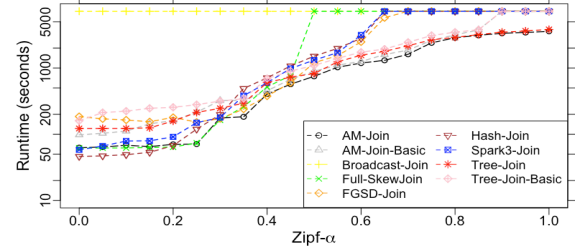


Figure 6: The runtime of the equi-join algorithms on 1000 executors for $D(\alpha, 1000)$ while varying the Zipf- α .

positive Integer space, and 10^7 records whose Zipfian keys have a range of 10^5 while varying the Zipf- α .

For these relatively small records, the runtimes of all the algorithms were comparable until Zipf- α reached 0.6 with a slight edge for Hash-Join until Zipf- α reached 0.15. For Zipf- α in the range $[0.2, 0.55]$, none of the algorithms was a consistent winner. AM-Join and Tree-Join and their basic counterparts had a clearer edge for Zipf- α at 0.65. Only they successfully executed the joins starting at 0.7.

The experiment was repeated with records of size 10^3 Bytes instead of 10^2 Bytes, and the results are reported in Fig. 6. For these relatively large records, the runtimes of all the algorithms were comparable until Zipf- α reached 0.3 with a slight edge for Hash-Join in the Zipf- α $[0.0, 0.15]$ range. For the Zipf- α $[0.2, 0.3]$ range, none of the algorithms was a consistent winner. AM-Join had the edge for Zipf- α above 0.35. Full-SkewJoin, Hash-Join, Spark3-Join and FGSD-Join could not finish within the deadline starting at Zipf- α of 0.5, 0.65, 0.65, and 0.7 respectively. Even AM-Join-Basic and Tree-Join-Basic did not scale for Zipf- α starting 0.9 since they could not fit all the relatively large records of the hottest key in the memory of one executor.

The runtime of all the algorithms increased as the data skew increased. Not only do some executors become more loaded than others, but also the size of the results increases. The only exception was FGSD-Join, whose runtime was very stable through the low to mid range of Zipf- α ($[0.0, 0.6]$ and $[0.0, 0.3]$ in Fig. 5 and Fig. 6, respectively). The sampling phase was costly, but useless in load-balancing when the data was not skewed. In the mid Zipf- α range, FGSD-Join allocated more executors to the hot keys than the simpler Hash-Join, and hence was faster. For higher Zipf- α , FGSD-Join was bottlenecked by assigning each of the hottest keys to a single executor.

AM-Join and Tree-Join scale almost linearly with the increased skewness, since they are able to distribute the load on the executors fairly evenly. Their basic counterparts still

scaled almost linearly but were slower, due to the bottleneck of building the initial index and splitting the hot keys in the first iteration. From Ineq. 3, their runtimes are expected to increase with ℓ_{max} , the frequency of the hottest key, which is impacted by Zipf- α . Meanwhile, Full-SkewJoin and Hash-Join perform relatively well for weakly skewed joins until both the joined relations become mildly skewed (at a Zipf- α of 0.6 and 0.4 in Fig. 5 and Fig. 6, respectively). For moderately skewed data, both algorithms failed to produce the results within the deadline, albeit for different reasons. Full-SkewJoin could not load the hot keys and all their records in the memory of all the executors, while the executors of Hash-Join were bottlenecked by the join results of the hottest keys.

The Hash-Join executes faster than the adaptive algorithms (AM-Join and Full-SkewJoin) for the majority of the weakly skewed range (Zipf- α [0.0, 0.6] and [0.0, 0.3] ranges in Fig. 5 and Fig. 6, respectively), since the adaptive algorithms are slowed down by computing the hot keys. However, the adaptive algorithms utilizing the Broadcast-Join to join the keys that are hot in only one of the joined relations pays off for more skewed data. For larger Zipf- α (Zipf- α of 0.65 and 0.45 in Fig. 5 and Fig. 6, respectively), Full-SkewJoin executed clearly faster than Hash-Join, and AM-Join executed significantly faster than both.

Since the data partitions are too big to fit in memory, and they are already of roughly equal sizes, Spark3-Join performed as a basic Sort-Merge-Join. This was comparable, but slightly slower than Hash-Join.

Broadcast-Join was never able to execute successfully, regardless of the data skew, since both datasets were too large to load into the memory of the executors. Broadcast-Join is a fast algorithm, but is not a scalable one. This is clear from comparing the runtimes of Full-SkewJoin in Fig. 5 and Fig. 6, respectively. Since Full-SkewJoin employs Broadcast-Join for the hot keys, it was able to handle more skewed data when the records were smaller (until Zipf- $\alpha = 0.65$ and 0.45 when the record sizes were 10^2 and 10^3 , respectively).

For Tree-Join(-Basic) and AM-Join(-Basic), there were regions of relative flattening of the runtime due to the step-wise increase in the number of iterations. This is clear in the α [0.5, 0.7] and [0.85, 1.0] ranges in Fig. 5, and in the α [0.55, 0.7] and [0.8, 1.0] ranges in Fig. 6. This is because the number of iterations is a function of ℓ_{max} which is impacted by Zipf- α .

8.1.2 Exploring the Equi-Join Parameter Space

Similar results were obtained for different parameters, e.g., scaling the keys by a multiplier to influence the join selectivity, using 10^8 Zipfian records¹⁰, using records of size 10^4 Bytes, or allocating 4 GB of memory per executor. For non-skewed data, Hash-Join was consistently the fastest and FGSD-Join was consistently the slowest. Full-SkewJoin was fast while it can fit the data in memory, and AM-Join and Tree-Join were fast and able to scale for various α values. The runtime of Spark3-Join closely tracked that of Hash-Join but was slightly slower.

We also evaluated these algorithms on Small-Large joins. The Broadcast-Join performed best, and so did Spark3-Join since it also morphed into a Broadcast-Join. Full-SkewJoin

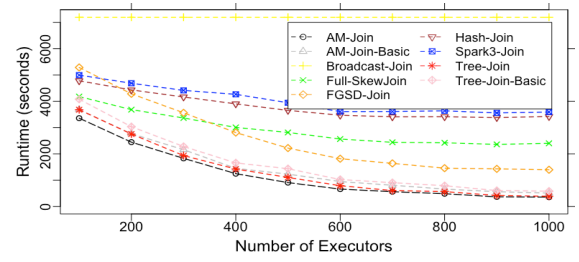


Figure 7: The runtime of the equi-join algorithms for $D(0.65, 100)$ while varying the number of executors.

performed slightly (11% to 15%) better than AM-Join, Tree-Join, FGSD-Join, and Hash-Join. As the size of the small relation increased and reached the memory limit, the Spark3-Join did not execute a Broadcast-Join, and the Broadcast-Join cannot accommodate the small relation in memory, and the results were very similar to those in § 8.1.1.

8.1.3 Equi-Join Scalability with Computational Resources

Fig. 7 shows the runtimes of the equi-join algorithms while varying the number of executors for two $D(0.65, 100)$ datasets. While the Zipf- α of 0.65 generates mildly skewed keys, this value was chosen, since this is the largest α where all the algorithms except Broadcast-Join were able to compute the join results.

All the algorithms, except Broadcast-Join, were able to scale with the increased number of resources. The algorithms showed a reduction in runtime as they were allowed more resources, albeit with various degrees. While FGSD-Join was the slowest at 100 executors, its runtime showed the biggest absolute drop. As the number of executors increased, the sample used by FGSD-Join to determine the key-ranges grew, allowing FGSD-Join to better distribute the load. The improvements of Hash-Join and Spark3-Join were the fastest to saturate, and their run-times almost did not improve starting at 700 executors, since the bottleneck was joining the hottest keys. Full-SkewJoin followed, and stopped having noticeable improvement at 800 executors. AM-Join(-Basic) and Tree-Join(-Basic) were able to improve their runtime as more executors were added, since they were able to split the load of joining the hottest keys among all the executors.

There is another phenomenon that is worth highlighting. The difference in the runtime between AM-Join, Tree-Join and their basic counterparts diminished as more executors were used. The reason is the majority of the scalability come from organizing the equi-join execution in multiple stages, which is shared by all the four algorithms.

Again, the Broadcast-Join was never able to execute successfully, regardless of the number of executors used, since neither of the datasets could be fit in the memory of the executors.

8.1.4 Speedup of Same-Attribute Self-Joins

We evaluate the speedup (calculated as the reduction ratio in runtime) gained by the optimizations in § 4.4. We report the Tree-Join speedup between joining a dataset with itself as a regular equi-join, and executing a same-attribute self-join (i.e., eliminating the redundant join results). The

¹⁰Using 1000 executors, each dataset took over 10 hours to generate.

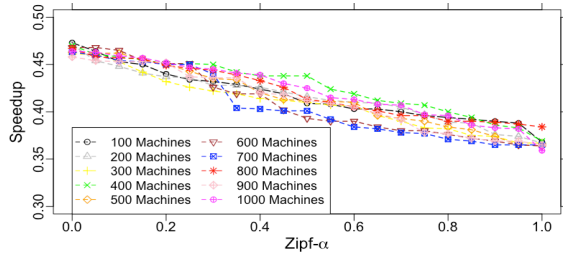


Figure 8: The same-attribute equi-join speedup of Tree-Join for $D(\alpha, 100)$ while varying the Zipf- α using various numbers of executors.

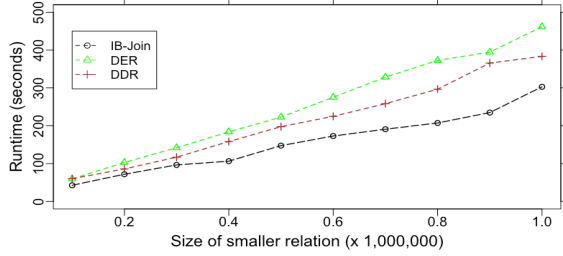


Figure 9: The runtime of the Small-Large outer-join algorithms while varying the size of the smaller relation.

speedup is reported only for Tree-Join, since AM-Join reduces to Tree-Join in the case of same-attribute self-joins. The speedups for different Zipf- α values using various numbers of executors are reported in Fig. 8. The experiments were run on a dataset with records of size 10^2 , but records of size 10^3 gave almost identical results.

From Fig. 8, the speedup was roughly 40% across the board regardless of the Zipf- α , and the number of executors. There are two observations to be made. First, the speedup decreased as the Zipf- α increased. This can be attributed to the number of Tree-Join iterations which are not impacted by the processing and IO savings discussed in § 4.4. The larger the Zipf- α , the more skewed the data, and the larger number of Tree-Join iterations. Scheduling these iterations is a fixed overhead does not enjoy the same savings discussed in § 4.4. The other observation is as the number of machines increased, the savings tended to decrease. This can be attributed to the fixed overhead of communication among the machines as their number increases.

8.1.5 Performance on Small-Large Outer-Joins

Fig. 9 shows the runtimes of IB-Join, DER [78] and DDR [24]¹¹ when performing a right-outer join of two relations with records of size 10^2 Bytes, and keys uniformly selected in the range $[1, 2 \times 10^5]$. The larger relation has 10^8 records, while the size of the smaller relation was varied between 10^5 and 10^6 records. The keys in the smaller relation were all even to ensure a selectivity of 50%. This is the selectivity that least favors the IB-Join family optimizations in § 5.1.

Fig. 9 confirms the communication cost analysis done in § 5.2. DDR was consistently faster than DER with one

¹¹For DER and DDR, the Spark implementations provided by the authors of [24] at <https://github.com/longcheng11/small-large> were used in these experiments.

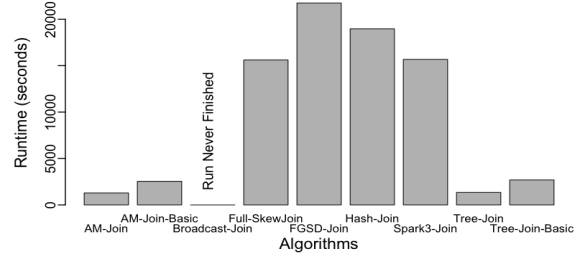


Figure 10: The runtime of the equi-join algorithms on 1000 executors on real data.

exception, while the right-outer variant of IB-Join was significantly faster than both. In reality, DER performs worse than shown in Fig. 9, since the time for assigning unique ids to the records is not shown.

8.2 Experiments on Real Data

We ran two experiments on real data. The first experiment was a same-attribute self-join on records collected from trips in a specific geo-location in October, 2020. The self-joined relation had 5.1×10^8 distinct keys, and each record was of size 36 Bytes. The total size of the data was 17.6 TB. Only AM-Join and Tree-Join were able to finish successfully. They both took 2.0 hours to finish. Full-SkewJoin, Hash-Join and Broadcast-Join did not finish in 48 hours.

The second experiment was a join between two relations. The first relation is the one described above. The second relation represented data on a single day, October 14th, 2020. The size of the second relation was 0.57 TB. The runtime of the equi-join algorithms on 1000 executors is shown in Fig. 10. All the algorithms, were able to finish successfully, except for Broadcast-Join since it could not fit the smaller relation in the memory of the executors. Thanks to organizing the equi-join execution in multiple stages, AM-Join and Tree-Join were able to execute an order of magnitude faster than all the other algorithms. Their basic counterparts however, executed significantly slower due to the load imbalance of building the initial index and splitting the hot keys in the first iteration.

9. CONCLUSION

This paper proposes Adaptive-Multistage-Join (AM-Join) a fast, efficient and scalable equi-join algorithm that is built using the basic MapReduce primitives, and is hence deployable in any distributed shared-nothing architecture. The paper started by proposing Tree-Join, a novel algorithm that organizes the equi-join execution in multiple stages. Tree-Join attains scalability by distributing the load of joining a key that is hot in both relations throughout the join execution. Such keys are the scalability bottleneck of most of the state-of-the-art distributed algorithms. AM-Join utilizes Tree-Join for load balancing, high resource utilization, and scalability. Moreover, AM-Join utilizes Broadcast-Joins that reduce the network load when joining keys that are hot in only one relation. By utilizing Tree-Join and Broadcast-Join, AM-Join achieves speed, efficiency, and scalability. AM-Join extends to all the outer-joins elegantly without record deduplication or custom table partitioning, unlike the state-of-the-art industry-scale algorithms [19]. For the fastest execution of AM-Join outer-joins, the paper proposed

Index-Broadcast-Join (IB-Join) family that improves on the state-of-the-art Small-Large outer-join algorithms [78, 24]. All the proposed algorithms use the basic MapReduce primitives only, and hence can be adopted on any shared-nothing architecture.

This paper also proposes a novel type of joins, same-attribute self-joins, which is at the intersection of equi-joins, inner-joins, and self-joins. The paper shows how to optimize Tree-Join to save roughly half the processing and IO when executing same-attribute self-joins.

All the theoretical claims have been verified using extensive evaluation. Our evaluation highlights the improved performance and scalability of AM-Join when applied to the general equi-joins. When compared to the state-of-the-art algorithms [19, 36], AM-Join executed comparably fast on weakly-skewed synthetic tables and can join more-skewed or orders-of-magnitude bigger tables, including our real-data tables. These advantages are even more pronounced when applying the join algorithms to same-attribute self-joins. The proposed IB-Join outer-join algorithm executed much faster than the state-of-the-art algorithms in [78, 24].

Our future directions focus on optimizing AM-Join for the general shared-nothing architecture that supports multicasting data, for NUMA machines connected by a high-bandwidth network, and learning from the RDMA and the work-stealing enhancements of [63]. Moreover, we plan to explore using Radix join [52, 12] that it is only bound by the memory bandwidth as the Shuffle-Join.

10. ACKNOWLEDGMENTS

We like to express our appreciation to Sriram Padmanabhan, Vijayasaradhi Uppaluri, Gaurav Bansal, and Ryan Stentz from Uber for revising the manuscript and improving the presentation of the algorithms, and to Nicolas Bruno from Microsoft for discussing the SkewJoin algorithms, and to Shixuan Fan from Snowflake for revising the theoretical foundations.

11. REFERENCES

- [1] F. Afrati, N. Stasinopoulos, J. Ullman, and A. Vassilakopoulos. SharesSkew: An Algorithm to Handle Skew for Joins in MapReduce. *Information Systems*, 77:129–150, 2018.
- [2] F. Afrati and J. Ullman. Optimizing Joins in a Map-Reduce Environment. In *EDBT International Conference on Extending Database Technology*, pages 99–110, 2010.
- [3] P. Agarwal, G. Cormode, Z. Huang, J. Phillips, Z. Wei, and K. Yi. Mergeable Summaries. *TODS ACM Transactions on Database Systems*, 38(4):1–28, 2013.
- [4] M.-C. Albutiu, A. Kemper, and T. Neumann. Massively Parallel Sort-Merge Joins in Main Memory Multi-Core Database Systems. *arXiv preprint arXiv:1207.0145*, 2012.
- [5] K. Alway and A. Nica. Constructing Join Histograms from Histograms with q-error Guarantees. In *ACM SIGMOD International Conference on Management of Data*, pages 2245–2246, 2016.
- [6] Apache Hadoop. <http://hadoop.apache.org>.
- [7] F. Atta, S. Viglas, and S. Niazi. SAND Join — A Skew Handling Join Algorithm for Google’s MapReduce Framework. In *IEEE INMIC International Multitopic Conference*, pages 170–175. IEEE, 2011.
- [8] C. Balkesen, G. Alonso, J. Teubner, and M. T. Özsu. Multi-Core, Main-Memory Joins: Sort vs. Hash Revisited. *Proceedings of the VLDB Endowment*, 7(1):85–96, 2013.
- [9] C. Balkesen, J. Teubner, G. Alonso, and M. T. Özsu. Main-Memory Hash Joins on Multi-Core CPUs: Tuning to the Underlying Hardware. In *IEEE ICDE International Conference on Data Engineering*, pages 362–373, 2013.
- [10] M. Bandle, J. Giceva, and T. Neumann. To Partition, or Not to Partition, That is the Join Question in a Real System. In *ACM SIGMOD International Conference on Management of Data*, pages 168–180, 2021.
- [11] A. Bar-Noy and S. Kipnis. Designing Broadcasting Algorithms in the Postal Model for Message-Passing Systems. *Mathematical Systems Theory*, 27(5):431–452, 1994.
- [12] C. Barthels, S. Loesing, G. Alonso, and D. Kossmann. Rack-Scale In-Memory Join Processing using RDMA. In *ACM SIGMOD International Conference on Management of Data*, pages 1463–1475, 2015.
- [13] C. Barthels, I. Müller, T. Schneider, G. Alonso, and T. Hoefer. Distributed Join Algorithms on Thousands of Cores. *Proceedings of the VLDB Endowment*, 10(5):517–528, 2017.
- [14] P. Bernstein, N. Goodman, E. Wong, C. Reeve, and J. Rothnie Jr. Query Processing in a System for Distributed Databases. *TODS ACM Transactions on Database Systems*, 6(4):602–625, 1981.
- [15] C. Binnig, A. Crotty, A. Galakatos, T. Kraska, and E. Zamanian. The End of Slow Networks: It’s Time for a Redesign. *Proceedings of the VLDB Endowment*, 9(7):528–539, 2016.
- [16] S. Blanas, Y. Li, and J. Patel. Design and Evaluation of Main Memory Hash Join Algorithms for Multi-core CPUs. In *ACM SIGMOD International Conference on Management of Data*, pages 37–48, 2011.
- [17] S. Blanas, J. Patel, V. Ercegovac, J. Rao, E. Shekita, and Y. Tian. A Comparison of Join Algorithms for Log Processing in MapReduce. In *ACM SIGMOD International Conference on Management of Data*, pages 975–986, 2010.
- [18] M. Blasgen and K. Eswaran. Storage and Access in Relational Data Bases. *IBM Systems Journal*, 16(4):363–377, 1977.
- [19] N. Bruno, Y. Kwon, and M.-C. Wu. Advanced Join Strategies for Large-Scale Distributed Computation. *Proceedings of the VLDB Endowment*, 7(13):1484–1495, 2014.
- [20] R. Chen and V. Prasanna. Accelerating Equi-Join on a CPU-FPGA Heterogeneous Platform. In *IEEE International Symposium on Field-Programmable Custom Computing Machines (FCCM)*, pages 212–219, 2016.
- [21] Z. Chen and A. Zhang. A Survey of Approximate Quantile Computation on Large-Scale Data. *IEEE Access*, 8:34585–34597, 2020.
- [22] L. Cheng, S. Kotoulas, T. Ward, and G. Theodoropoulos. QbDJ: A Novel Framework for Handling Skew in Parallel Join Processing on

- Distributed Memory. In *IEEE HPCC International Conference on High Performance Computing and Communications*, pages 1519–1527. IEEE, 2013.
- [23] L. Cheng, S. Kotoulas, T. Ward, and G. Theodoropoulos. Robust and Skew-resistant Parallel Joins in Shared-Nothing Systems. In *ACM CIKM International Conference on Conference on Information and Knowledge Management*, pages 1399–1408, 2014.
- [24] L. Cheng, I. Tachmazidis, S. Kotoulas, and G. Antoniou. Design and Evaluation of Small-Large Outer Joins in Cloud Computing Environments. *Journal of Parallel and Distributed Computing*, 110:2–15, 2017.
- [25] T.-Y. Cheung. A Method for Equijoin Queries in Distributed Relational Databases. *IEEE TOC Transactions on Computers*, 100(8):746–751, 1982.
- [26] S. Chu, M. Balazinska, and D. Suciu. From theory to practice: Efficient join query evaluation in a parallel database system. In *ACM SIGMOD International Conference on Management of Data*, pages 63–78, 2015.
- [27] E. Codd. A Relational Model of Data for Large Shared Data Banks. *Communications of the ACM*, 13(6):377–387, 1970.
- [28] E. Codd. Relational Completeness of Data Base Sublanguages. In *Database Systems, R. Rustin (ed.)*, pages 65–98. Prentice Hall, Englewood Cliffs, NJ, USA, 1972.
- [29] G. Cormode and P. Vesely. A Tight Lower Bound for Comparison-Based Quantile Summaries. In *ACM PODS SIGMOD-SIGACT-SIGAI Symposium on Principles of Database Systems*, pages 81–93, 2020.
- [30] A. Das, J. Gehrke, and M. Riedewald. Approximate Join Processing over Data Streams. In *ACM SIGMOD International Conference on Management of Data*, pages 40–51, 2003.
- [31] G. Date. The Outer Join. In *International Conference of Databases*, pages 76–106, 1983.
- [32] J. Dean and S. Ghemawat. MapReduce: Simplified Data Processing on Large Clusters. *Communications of the ACM*, 51(1):107–113, 2008.
- [33] D. DeWitt, S. Ghandeharizadeh, D. Schneider, A. Bricker, H. Hsiao, and R. Rasmussen. The Gamma Database Machine Project. *IEEE TKDE Transactions on Knowledge and Data Engineering*, 2(1):44–62, 1990.
- [34] D. DeWitt, J. Naughton, D. Schneider, and S. Seshadri. Practical Skew Handling in Parallel Joins. Technical report, University of Wisconsin-Madison Department of Computer Sciences, 1992.
- [35] D. DeWitt, M. Smith, and H. Borat. A Single-User Performance Evaluation of the Teradata Database Machine. In *International Workshop on High Performance Transaction Systems*, pages 243–276. Springer, 1987.
- [36] E. Gavagsaz, A. Rezaee, and H. Javadi. Load Balancing in Join Algorithms for Skewed Data in MapReduce Systems. *The Journal of Supercomputing*, 75(1):228–254, 2019.
- [37] G. Graefe. Sort-Merge-Join: An Idea Whose Time Has(h) Passed? In *IEEE ICDE International Conference on Data Engineering*, pages 406–417. IEEE, 1994.
- [38] V. Gulisano, Y. Nikolakopoulos, M. Papatriantafyllou, and P. Tsigas. ScaleJoin: a Deterministic, Disjoint-Parallel and Skew-Resilient Stream Join. *IEEE Transactions on Big Data*, 7(2):299–312, 2016.
- [39] C. Guo, H. Chen, F. Zhang, and C. Li. Distributed Join Algorithms on Multi-CPU Clusters with GPUDirect RDMA. In *ICPP International Conference on Parallel Processing*, pages 1–10, 2019.
- [40] M. Hassan and M. Bamha. An Efficient Parallel Algorithm for Evaluating Join Queries on Heterogeneous Distributed Systems. In *IEEE HiPC International Conference on High Performance Computing*, pages 350–358. IEEE, 2009.
- [41] B. He, K. Yang, R. Fang, M. Lu, N. Govindaraju, Q. Luo, and P. Sander. Relational Joins on Graphics Processors. In *ACM SIGMOD International Conference on Management of Data*, pages 511–524, 2008.
- [42] J. Hursch. Relational Joins: More than Meets the Eye. *Database Program Design*, 2(12):64–70, 1989.
- [43] D. Jiang, A. Tung, and G. Chen. MAP-JOIN-REDUCE: Toward Scalable and Efficient Data Analysis on Large Clusters. *IEEE TKDE Transactions on Knowledge and Data Engineering*, 23(9):1299–1311, 2010.
- [44] T. Kaldewey, G. Lohman, R. Mueller, and P. Volk. GPU Join Processing Revisited. In *International Workshop on Data Management on New Hardware*, pages 55–62, 2012.
- [45] C. Kim, T. Kaldewey, V. Lee, E. Sedlar, A. Nguyen, N. Satish, J. Chhugani, A. D. Blas, and P. Dubey. Sort vs. Hash Revisited: Fast Join Implementation on Modern Multi-Core CPUs. *Proceedings of the VLDB Endowment*, 2(2):1378–1389, 2009.
- [46] M. Kitsuregawa, H. Tanaka, and T. Moto-Oka. Application of Hash to Data Base Machine and its Architecture. *New Generation Computing*, 1(1):63–74, 1983.
- [47] M. Lakshmi and P. Yu. Effectiveness of Parallel Joins. *IEEE Computer Architecture Letters*, 2(04):410–424, 1990.
- [48] R. Lämmel. Google’s MapReduce programming model — Revisited. *Science of Computer Programming*, 70(1):1–30, 2008.
- [49] F. Li, S. Das, M. Syamala, and V. Narasayya. Accelerating Relational Databases by Leveraging Remote Memory and RDMA. In *ACM SIGMOD International Conference on Management of Data*, pages 355–370, 2016.
- [50] Q. Lin, B. Ooi, Z. Wang, and C. Yu. Scalable Distributed Stream Join Processing. In *ACM SIGMOD International Conference on Management of Data*, pages 811–825, 2015.
- [51] J. Linn and C. Dyer. Data-Intensive Text Processing with MapReduce. *Synthesis Lectures on Human Language Technologies*, 3(1):1–177, 2010.
- [52] S. Manegold, P. Boncz, and M. Kersten. Optimizing Main-Memory Join on Modern Hardware. *IEEE TKDE Transactions on Knowledge and Data Engineering*, 14(4):709–730, 2002.
- [53] A. Metwally. Scaling Equi-Joins. In *ACM SIGMOD*

- International Conference on Management of Data*, pages 2163–2176, 2022.
- [54] A. Metwally, D. Agrawal, and A. E. Abbadi. Efficient Computation of Frequent and Top-k Elements in Data Streams. In *ICDT International Conference on Database Theory*, pages 398–412. Springer, 2005.
 - [55] A. Metwally and C. Faloutsos. V-SMART-Join: A Scalable MapReduce Framework for All-Pair Similarity Joins of Multisets and Vectors. *Proceedings of the VLDB Endowment*, 5(8):704–715, 2012.
 - [56] A. Nica, I. Charlesworth, and M. Panju. Analyzing Query Optimization Process: Portraits of Join Enumeration Algorithms. In *IEEE ICDE International Conference on Data Engineering*, pages 1301–1304. IEEE, 2012.
 - [57] A. Okcan and M. Riedewald. Processing Theta-Joins using MapReduce. In *ACM SIGMOD International Conference on Management of Data*, pages 949–960, 2011.
 - [58] J. Paul, B. He, S. Lu, and C. Lau. Revisiting Hash Join on Graphics Processors: A Decade Later. *Distributed and Parallel Databases*, pages 1–23, 2020.
 - [59] J. Paul, S. Lu, B. He, and C. Lau. MG-Join: A Scalable Join for Massively Parallel Multi-GPU Architectures. In *ACM SIGMOD International Conference on Management of Data*, pages 1413–1425, 2021.
 - [60] O. Polychroniou, W. Zhang, and K. Ross. Track Join: Distributed Joins with Minimal Network Traffic. In *ACM SIGMOD International Conference on Management of Data*, pages 1483–1494, 2014.
 - [61] O. Polychroniou, W. Zhang, and K. Ross. Distributed Joins and Data Placement for Minimal Network Traffic. *TODS ACM Transactions on Database Systems*, 43(3):1–45, 2018.
 - [62] D. Quoc, I. Akkus, P. Bhatotia, S. Blanas, R. Chen, C. Fetzer, and T. Strufe. ApproxJoin: Approximate Distributed Joins. In *ACM SoCC Symposium on Cloud Computing*, pages 426–438, 2018.
 - [63] W. Rödiger, S. Idicula, A. Kemper, and T. Neumann. Flow-Join: Adaptive Skew Handling for Distributed Joins over High-Speed Networks. In *IEEE ICDE International Conference on Data Engineering*, pages 1194–1205. IEEE, 2016.
 - [64] W. Rödiger, T. Mühlbauer, A. Kemper, and T. Neumann. High-Speed Query Processing over High-Speed Networks. *Proceedings of the VLDB Endowment*, 9(4):228–239, 2015.
 - [65] R. Rui, H. Li, and Y.-C. Tu. Efficient Join Algorithms For Large Database Tables in a Multi-GPU Environment. *Proceedings of the VLDB Endowment*, 14(4):708–720, 2020.
 - [66] A. Salama, C. Binnig, T. Kraska, A. Scherp, and T. Ziegler. Rethinking Distributed Query Execution on High-Speed Networks. *IEEE Data Engineering Bulletin*, 40(1):27–37, 2017.
 - [67] P. Sanders, J. Speck, and J. Träff. Two-Tree Algorithms for Full Bandwidth Broadcast, Reduction and Scan. *Parallel Computing*, 35(12):581–594, 2009.
 - [68] D. Schneider and D. DeWitt. A Performance Evaluation of Four Parallel Join Algorithms in a Shared-Nothing Multiprocessor Environment. *ACM SIGMOD Record*, 18(2):110–121, 1989.
 - [69] S. Schuh, X. Chen, and J. Dittrich. An Experimental Comparison of Thirteen Relational Equi-Joins in Main Memory. In *ACM SIGMOD International Conference on Management of Data*, pages 1961–1976, 2016.
 - [70] P. Selinger, M. Astrahan, D. Chamberlin, R. Lorie, and T. Price. Access Path Selection in a Relational Database Management System. In *ACM SIGMOD International Conference on Management of Data*, pages 23–34, 1979.
 - [71] D. Shasha and T.-L. Wang. Optimizing Equijoin Queries In Distributed Databases Where Relations Are Hash Partitioned. *TODS ACM Transactions on Database Systems*, 16(2):279–308, 1991.
 - [72] P. Sioulas, P. Chrysogelos, M. Karpathiotakis, R. Appuswamy, and A. Ailamaki. Hardware-conscious Hash-Joins on GPUs. In *IEEE ICDE International Conference on Data Engineering*, pages 698–709, 2019.
 - [73] M. Stonebraker. The Case for Shared Nothing. *IEEE Database Engineering Bulletin*, 9(1):4–9, 1986.
 - [74] S. Suri and S. Vassilvitskii. Counting Triangles and the Curse of the Last Reducer. In *WWW International Conference on World Wide Web*, pages 607–614, 2011.
 - [75] Y. Tian, F. Özcan, T. Zou, R. Goncalves, and H. Pirahesh. Building a Hybrid Warehouse: Efficient Joins Between Data Stored in HDFS and Enterprise Warehouse. *TODS ACM Transactions on Database Systems*, 41(4):1–38, 2016.
 - [76] A. Vitorovic, M. Elseidy, and C. Koch. Load Balancing and Skew Resilience for Parallel Joins. In *IEEE ICDE International Conference on Data Engineering*, pages 313–324. IEEE, 2016.
 - [77] Word frequency in Wikipedia (November 27, 2006). https://en.wikipedia.org/wiki/Zipf's_law.
 - [78] Y. Xu and P. Kostamaa. A New Algorithm for Small-Large Table Outer Joins in Parallel DBMS. In *IEEE ICDE International Conference on Data Engineering*, pages 1018–1024. IEEE, 2010.
 - [79] Y. Xu, P. Kostamaa, X. Zhou, and L. Chen. Handling Data Skew in Parallel Joins in Shared-Nothing Systems. In *ACM SIGMOD International Conference on Management of Data*, pages 1043–1052, 2008.
 - [80] H.-C. Yang, A. Dasdan, R.-L. Hsiao, and D. Parker. Map-Reduce-Merge: Simplified Relational Data Processing on Large Clusters. In *ACM SIGMOD International Conference on Management of Data*, pages 1029–1040, 2007.
 - [81] K. Yi and Q. Zhang. Optimal Tracking of Distributed Heavy Hitters and Quantiles. *Algorithmica*, 65(1):206–223, 2013.
 - [82] M. Zaharia, M. Chowdhury, M. Franklin, S. Shenker, and I. Stoica. Spark: Cluster Computing with Working Sets. *HotCloud*, 10(10-10):95, 2010.